Title

Synthesis and Characterization of $NiFe_2O_4$/g-C_3N_4/ZnO Heterogeneous Photocatalytic Nanocomposites and Their Applications For Dye Degradation and Water Splitting

Name: Saman Aqeel

Registration no.: 00000203282

A dissertation submitted in partial fulfillment of the requirements for the Degree of Master of Science in Chemistry

Supervisor: Dr. Azhar Mahmood

FORM TH-4

National University of Sciences & Technology

MS THESIS WORK

We hereby recommend that the dissertation prepared under our supervision by: Saman Aqeel, Regn No. 00000203282 Titled: Synthesis and Characterization of NiFe204/g-C3N4/Zno Heterogenous Photocatalytic nanocomposites and their applications for Dye Degradation and Water Splitting be accepted in partial fulfillment of the requirements for the award of **MS** degree.

Examination Committee Members

1. Name: DR. MUDASSIR IQBAL Signature: _____

2. Name: DR. MANZAR SOHAIL Signature: _____

External Examiner: DR. SHAHID IQBAL Signature: _____

Supervisor's Name DR. AZHAR MAHMOOD Signature: _____

_____ 07/11/19
Head of Department Date

COUNTERSINGED

Date: 07/11/19 07/11/2019
Dean/Principal

THESIS ACCEPTANCE CERTIFICATE

Certified that final copy of MS thesis written by **Ms. Saman Aqeel,** (Registration No. **00000203282**), of **School of Natural Sciences** has been vetted by undersigned, found complete in all respects as per NUST statutes/regulations, is free of plagiarism, errors, and mistakes and is accepted as partial fulfillment for award of MS/M.Phil degree. It is further certified that necessary amendments as pointed out by GEC members and external examiner of the scholar have also been incorporated in the said thesis.

Signature: _____

Name of Supervisor: Dr. Azhar mahmood

Date: 7/11/19

Signature (HoD): _____

Date: 07/11/19

Signature (Dean/Principal): _____

Date: 07/11/19

Department of Chemistry

School of Natural Sciences (SNS)

National University of Science and Technology (NUST)

H-12 Islamabad, Pakistan

2019

Dedication

This thesis is dedicated to my beloved parents Mr. Aqeel Ahmed and Mrs. Samina Aqeel

Acknowledgments

I would like to thank ***Allah Almighty***, who has given me the courage and ability to complete this thesis and gave me strength throughout my research work.

My sincere thanks to my supervisor, ***Dr. Azhar Mahmood*** who guided me well throughout my research work and also listened to my problems and provided me the best possible solution for every problem. I am also thankful to my GEC members ***Dr. Manzar Sohail*** and ***Dr. Muddasir Iqbal*** for their guidance and suggestions during my research period. I also acknowledge the services of ***School of Natural Sciences, NUST*** for providing me due facilities and a comfortable environment to work. I am also grateful for the technical support provided by ***IESE, CASEN*** and ***SCME*** from among NUST and other institutes such as ***National Centre for Physics.*** I would also like to express my gratitude to my friends who supported in my research work and providing me with guidance and required assistance. I would also like to thank my family members for the support and assistance they have provided me during my journey.

Saman Aqeel

Abstract

In this study, nanomaterials of $NiFe_2O_4$ and ZnO were synthesized by hydrothermal methods and g-C_3N_4 was synthesized by calcination in furnace. Subsequently, ternary composite of these components were prepared by solid state mixing in different ratios like 1:1:1, 1:3:1, and 3:1:1 w/w of $NiFe_2O_4$, g-C_3N_4 and ZnO as synthesized materials respectively.

The synthesized nanocomposites were characterized by SEM and XRD while DRS was also carried out to find out their energy band gaps. The SEM depicted the morphology of the sample with perfect crystallite size. $NiFe_2O_4$ had a perfect rectangular plates like structure while g-C_3N_4 was a layered material because of the presence of graphene. ZnO was agglomerated in a beautiful flower shaped pattern and the nano composite of all the three materials appeared in the form of a sandwich with the layering of g-C_3N_4 and ZnO on the rectangular $NiFe_2O_4$ plates.

The XRD revealed the tetragonal planes for $NiFe_2O_4$ and the hexagonal planes for ZnO while the g-C_3N_4 showed the diffraction planes with no extra peaks present in the sample which indicated the purity of the sample.

Degradation studies of the dye methyl orange were carried out by UV-VIS spectrophotometer with highest degradation efficiency of 78% by composite 1:1:1 which showed the best activity. The degradation efficiency of 1:3:1 and 3:1:1 was 33% and 19% respectively.

Water splitting was carried out by CV technique in the presence of KOH where the conductivity increased by increasing scan rate and current which indicated the stability and uniformity of the nano composite.

Table of Contents

List of Abbreviations

$NiFe_2O_4$	Nickle Ferrite
g-C_3N_4	Graphitic carbon nitride
ZnO	Zinc oxide
SEM	Scanning electron microscope
XRD	X-Ray Diffraction
UV-VIS	Ultraviolet visible spectroscopy
DRS	Diffuse reflectance spectroscopy
eV	electron volt
nm	nano meter
M	Molarity
g/mol	gram per mole
hr.	hour
Conc.	Concentration
^oC	degree centigrade
NaOH	sodium hydroxide
e^-	Electron
h^+	hole
CB	conduction band
VB	valence band
H_2	hydrogen
·OH	hydroxyl radical
CO_2	carbon dioxide

Chapter 1: Introduction

1.1. Background

Scientists and researchers have been working from many years to look for an environmental friendly material and techniques for the removal of pollutants and hazardous substances from air, soil and water [1]. Water is one of most important and necessary compound present on earth without which life cannot survive. Body physiological processes such as respiration and sweating carry out a lot of water loss so a constant water supply is required to replace this lost water [2]. However, the water utilized by human beings need to be clean and pure. The cleanliness of water is a grave problem these days as they contain hazardous and toxic materials such as pesticides, herbicides, dyes, heavy metals and organic toxins. Most of these chemicals are very harmful and even carcinogenic and in countries like Pakistan are dumped directly into the fresh water which can affect the human as well as animal and marine life [3].

Dyes are present in the discharged wastes that are lethal to life of human beings, marine life and microorganisms. During the dyeing procedure, about 1-20% of the total dye is released in water [4]. These colored waste waters released are a major source of eutrophication and grave water pollution and by different chemical reactions in the wastewater phase and even by hydrolysis and oxidation are harmful byproducts of waste water released [5].

Two key components are present in dye molecules. The first one responsible for the color is called chromophore, and the second one name auxochrome not just supplement chromophore but also makes the molecule soluble [6]. As small as 1.0mg/L of the dye could impart significant color to the water and making I harmful for human consumption. Dyes are extremely dangerous and may be carcinogenic or mutagenic and may effect human beings in severe way like damage to central nervous system and brain functioning as well as effecting functions of kidneys, liver and reproductive system [7].

Many methods have been proposed in dye degradation including conventional physical procedures like ultrafiltration and adsorption, ion exchange and reverse osmosis are being used for many years for the removal of dyes from water [8]. These methods are not very efficient anymore due to their resistance to chemical as well as organic degradation as they carry out shift of dye from water to any other phase

causing secondary pollution. However, this further tiresome as require more financial support and energy [9]. However, these methods have been replaced by photochemical dye degradation and consume solar energy which is environmental friendly. Many such methods such as hydrogen production and carbon dioxide production are being used recently [10].

Today's world is all about increasing demand of energy and this has caused the attention of all the researchers towards the synthesis and storage of renewable energy such as that from hydrogen based fuels which can be obtained by water splitting [11]. Water splitting via electrochemical and photo electrochemical processes produces electrons and protons which combine together to reduce hydrogen and also oxygen as side product [12]. This provides a way to solve energy crisis and environmental issues while exploiting earth abundant water and also the sunlight available.

1.2. Photocatalysis

An advanced oxidation process used for degradation of dyes n other organic pollutants. Photocatalytic activity in this case depends upon the capability of catalyst to generate electron-hole pairs which create free radicals which are responsible for secondary reactions [13]. However, degradation of toxic pollutants in water can be carried out by heterogeneous photo catalysis where the reaction occurred by the incident light on the surface of the catalyst [14]. They not only are cost effective but also provide good results.

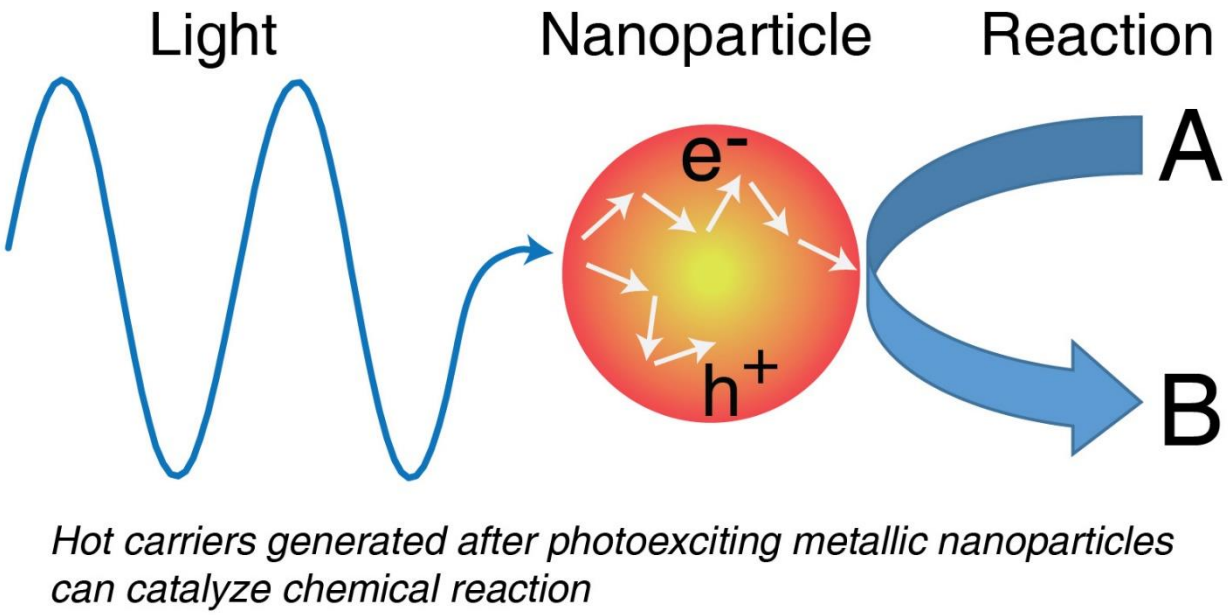

Figure 1: Overview of Photocatalysis

1.3. Properties of semiconductor Photo catalysts:

In a good and promising semiconductor, the valence state of the core element can be changed reversibly and also the hole can be accommodated without the decomposition of photo catalyst. In order to avoid the decomposition of holes, the element in the semiconductor must have at least one stable valence shell [15]. The semiconductor must be environmental friendly and cost effective.

1.4. Mechanism of Photo catalysis:

There is no sequence of electronic states as there was that in a semiconductor as there is in a metal but they have a free region ranging from highest occupied molecular orbital (HOMO) to lowest unoccupied molecular orbital (LUMO) which is also known as the band gap [16]. A photon is absorbed when the semiconductor is illuminated with light and a creation of hole occurs in VB due to a shift of electron from VB to CB only when the energy of the hole increases or becomes equal to that of band gap [17].

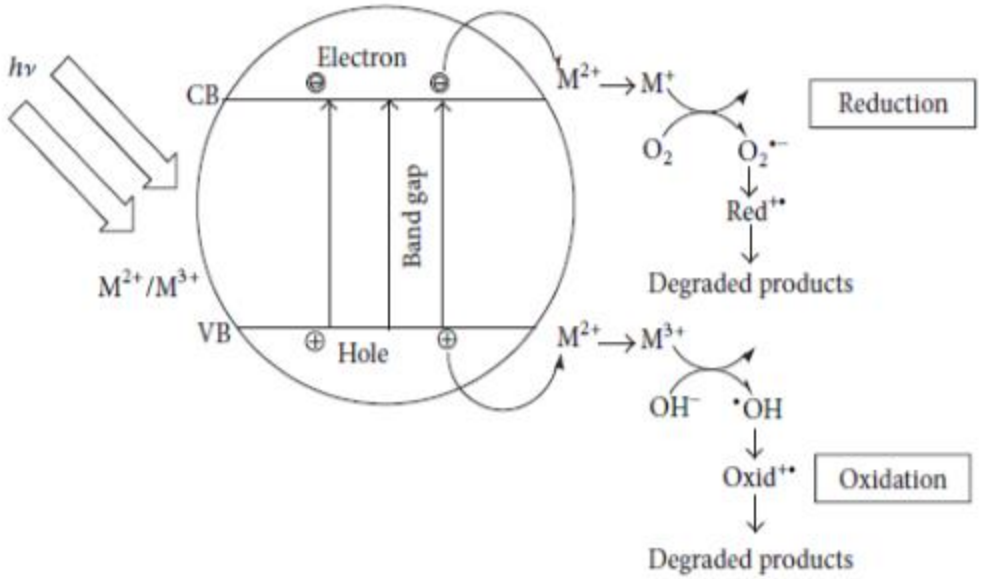

Figure 2: Diagrammatic illustration of mechanism of photo catalysis

The electron-hole pair shifts to the outer surface of the photo catalysts where it can get trapped in a metastable and release its energy as heat and may recombine with electrons donor and acceptors which are already adsorbed on the surface of semiconductor [18]. Oxidation of water occurs by the hole and this produces hydroxyl radicals which initiates a chain reaction. Oxidation is caused by this chain reaction and the generated electron maybe donated to the existing electron acceptor, for example, super oxides are formed as a result of this reaction from oxygen and are reduced to lower valence state [19]. Many semiconductors are used as photo catalysts including TiO_2, ZnO, Bi_2O_3, etc but g-C_3N_4 with a combination of $NiFe_2O_4$ supported on ZnO makes a very effective photocatalytic composite which is a heterogeneous composite and have distinctive physical aspects [20].

1.5. Nickel Ferrite:

One of the soft magnetic materials named nickel ferrite is one of the most auspicious class of materials due to its phenomenal properties and applications in catalysis and sensors. Nickel ferrite is one of the magnetic nanoparticles and possess an inverse spinal structure. This magnetic property is due to the divalent cations of Ni^{+2} in the crystal structure [21].

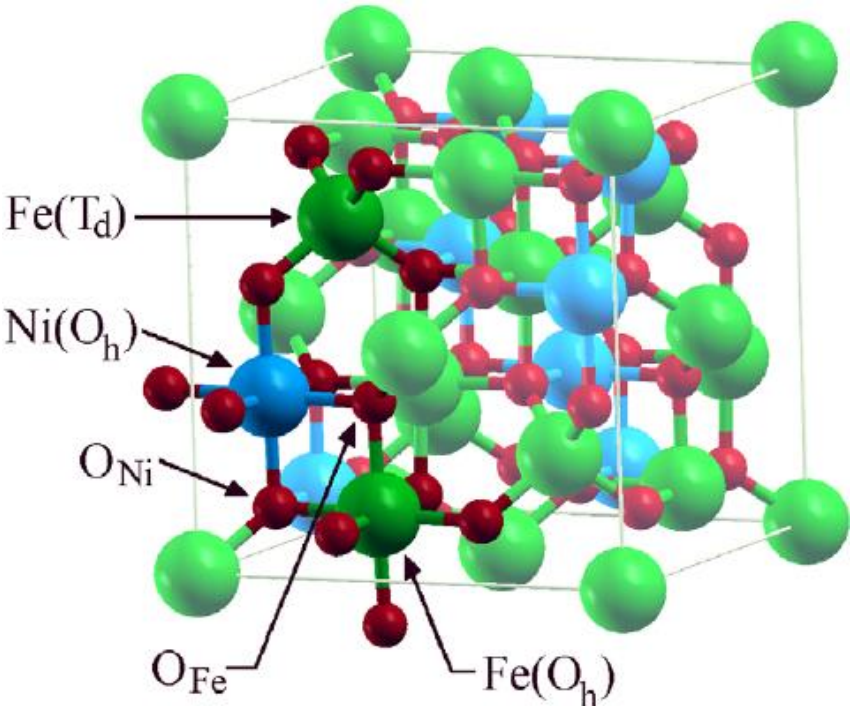

Figure 3: Inverse spinal unit cell of $NiFe_2O_4$

The composition and microstructure influences the properties of synthesized material which are also sensitive of the methodology of preparation of that material [22]. Various methods are involved in its synthesis sol-gel method, thermal decomposition method, hydrothermal method, co-precipitation method, thermolysis, microemulsion, and in the list include many more which has been employed for the preparation of nanocrystallite nickel ferrite [23].

1.6. Graphitic carbon nitride (g-C_3N_4) as photo catalyst:

g-C_3N_4 is a metal free polymer and is a n-type semiconductor. It possesses many promising optical properties which include optical, structural, electrical and physiochemical which are used in many technical applications such as catalytic and energy applications [24]. Graphitic carbon nitride gained fame when it led to the discovery of photocatalytic H_2 and O_2 in 2009. Therefore, g-C_3N_4 is emerging with many applications specially relating to water splitting and environmental pollutants degradation [25].

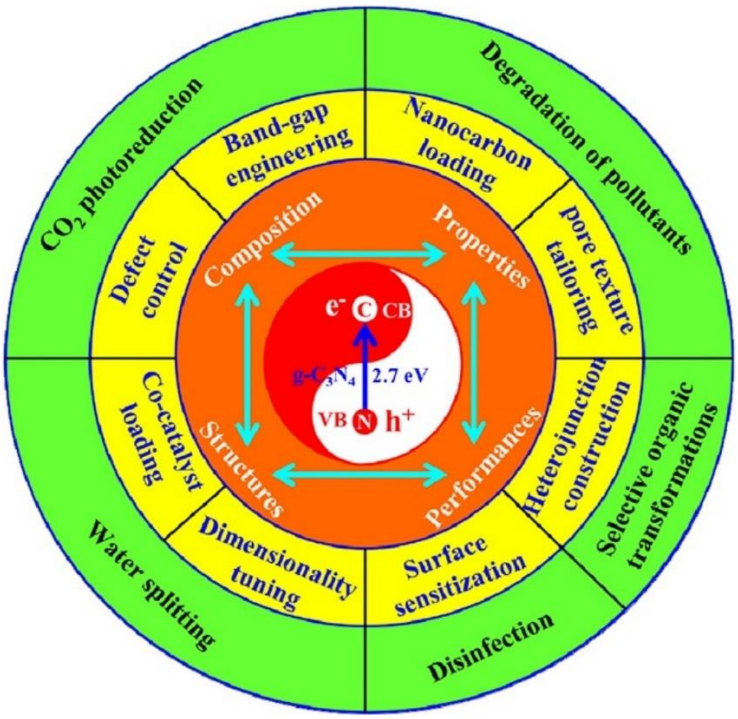

Figure 4: strategies and applications of g-C_3N_4 based photocatalyst

This is also used for the preparation of hybrid catalysts with various compositions, sixes, morphology, pore structure, thickness etc. Many nano catalysts in the form of 1D nano rods, 2D nano sheets, and 3D hierarchical structures have been extensively developed from g-C_3N_4 due to their efficient absorption of solar radiation, exposed active sites and large surface area [26].

The band gap of graphitic carbon nitride is 2.7ev in correspondence to a wavelength of 460nm which means it is active under visible light [27]. Graphitic carbon nitride has a suitable CB for various reduction reactions and its photo-generated electrons has large thermodynamic force for many small molecules like H_2O, CO_2 etc to generate H_2, O_2 etc. therefore, the electronic band structures of g-C_3N_4 are favorable enough for various applications in many fields like water slitting, pollutant degradation and disinfection [28].

1.7. ZnO as photo catalyst:

Due to excellent physical and chemical properties, zinc oxide nanoparticles are widely used in photocatalysis and also environmental applications. ZnO can be suitable alternative to TiO_2 for the photodegradation of pollutants due to their similar

band gap and photodegradation mechanism [29]. However, ZnO has higher photodegradation activity due to higher absorbance of light. The properties of ZnO depends upon not just the size and shape of nanostructure but also upon the purity of this material. There are various methods for the preparation of ZnO including thermal evaporation, laser ablation and as well as solution based methods like forced hydrolysis [30]. Modification of ZnO can also be carried out with various metals like Fe, Ni, Cu etc. The structural properties of ZnO including size, shape, morphology, and chemical composition can be altered by heat treatment resulting in change and sometimes improvement in photocatalytic activity [31].

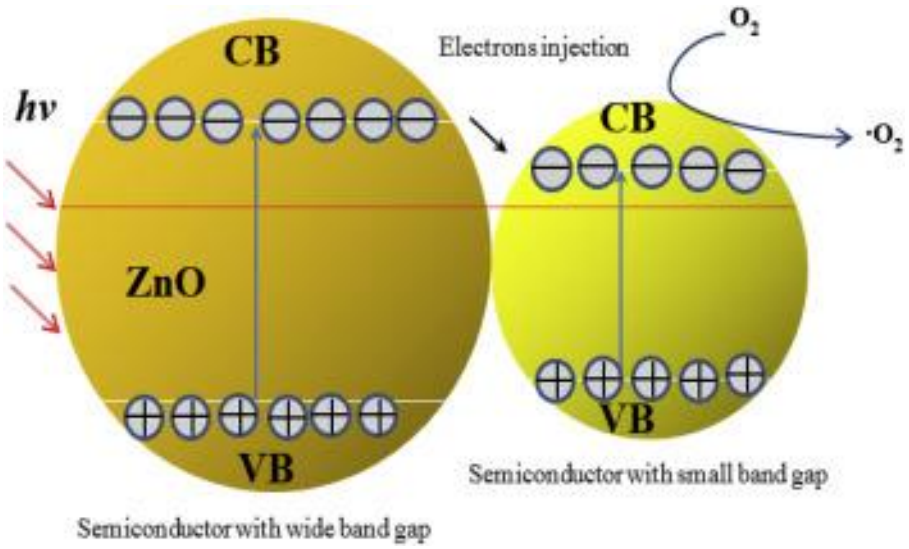

Figure 5: mechanism of ZnO transition

1.8. Common techniques for synthesis of compounds:

a) Hydrothermal Methods
b) Co-Precipitation method
c) Sol-gel method

Hydrothermal Method:

It is a very common method in which the nanoparticles of any compound are formed under high temperature and pressure in a solvent mostly water in a closed system so this procedure is precisely environmental friendly. Depending upon the parameters and the conditions, a large number of crystals can be formed. Finally, the product obtained is filtered, centrifuge, washed and annealed at proper temperature.

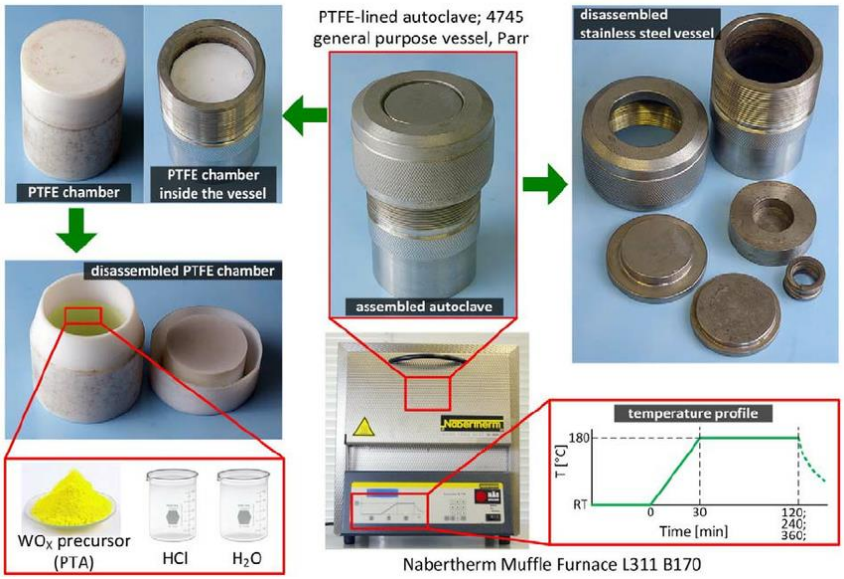

Figure 6: Hydrothermal synthesis set up

1.8.1. Co-Precipitation Method:

This is carried out by precipitation of different compounds which are soluble in one single solvent under particular condition. By fluctuation of temperature of reaction and also using the surface modification, the size of the nanoparticles can be properly controlled. Nanoparticles of size 30nm-100nm are produced by reaction of metal salt with a base in aqueous media by using mild oxidant. Cations conc., pH of the solution and presence of counter ions are the factors on which size and phase of sample particles depend. The average size of nanoparticles usually ranging from 15nm-2nm are mostly controlled by ionic strength and change in pH of the solution [32].

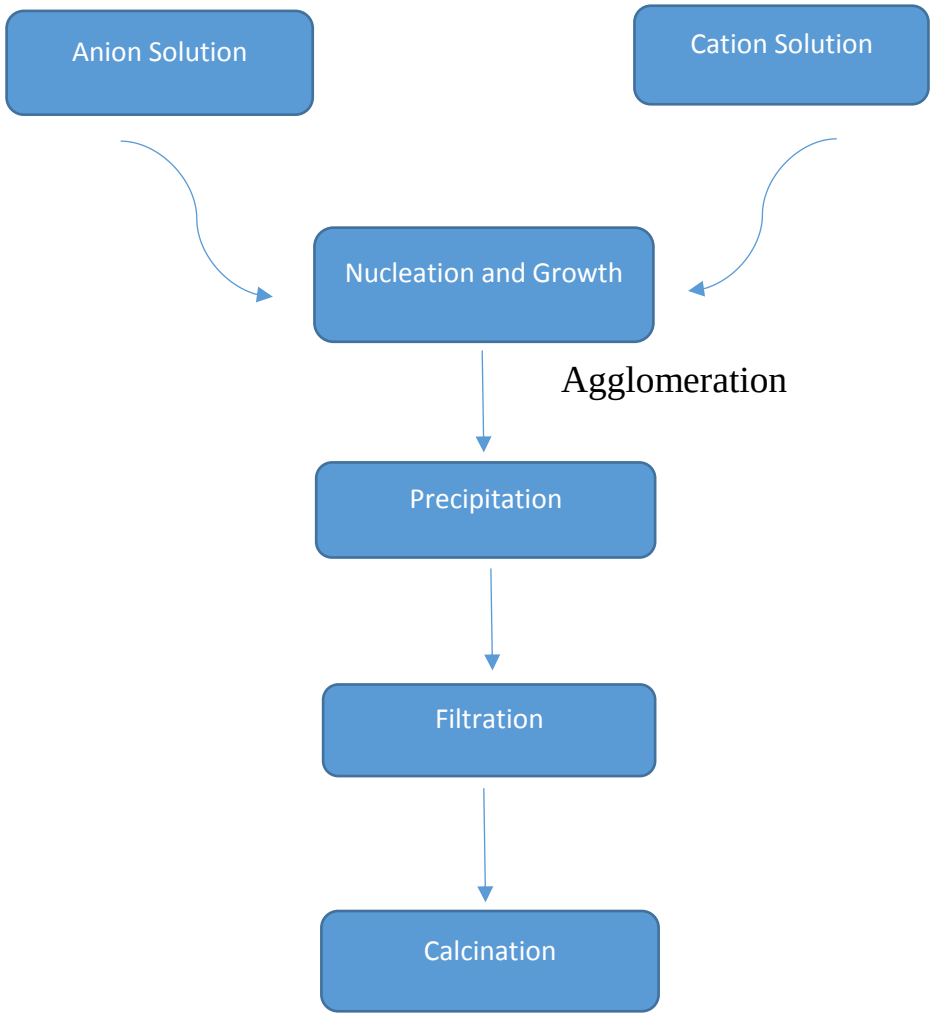

Figure 7: Methodology of Co-Precipitation

1.8.2. Sol-gel Method:

This technique involves the condensation and hydroxylation of molecular precursors in the solution. Sol is dried or converted to gel either by any chemical reaction to get desired metal oxide framework or by removing the solvent from it. A base or acid maybe used to hydrolyze the precursors but mostly water is used as a solvent. To obtain final crystalline form, heat is required otherwise the whole process takes place at room temperature.

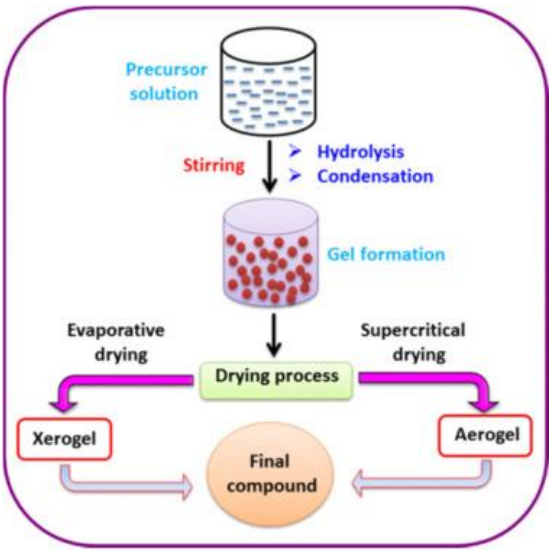

Figure 8: Sol-gel Methodology

1.8.3. Sonochemical Method:

Ultrasonic bath is used in this method to synthesize nanoparticles. A solution of a suitable solvent either ethanol or water and the metal oxide precursor is stirred properly for about 2 to 3 hours at room temperature. This solution is then placed in the sonication bath for certain time under certain temperature. Lastly, the solution is centrifuged, filtered and dried to obtain final nanoparticles product.

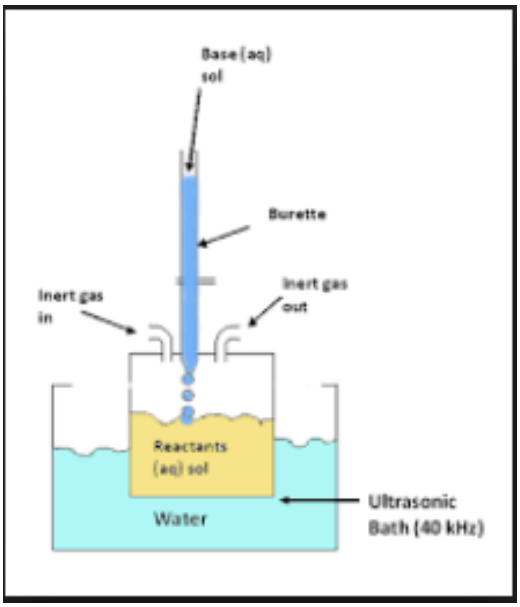

Figure 9: Ultra sonication bath

1.8.4. Chemical Vapor Deposition:

The solution in the vapor phase is condensed to acquire a solid product in this method. This process is used to alter electrical, mechanical, optical and thermal properties by the help of coatings. Deposition process takes place as a result thermal energy used to heat the gas in the chamber. Nanoparticles of articular material can be achieved under well-defined conditions [33].

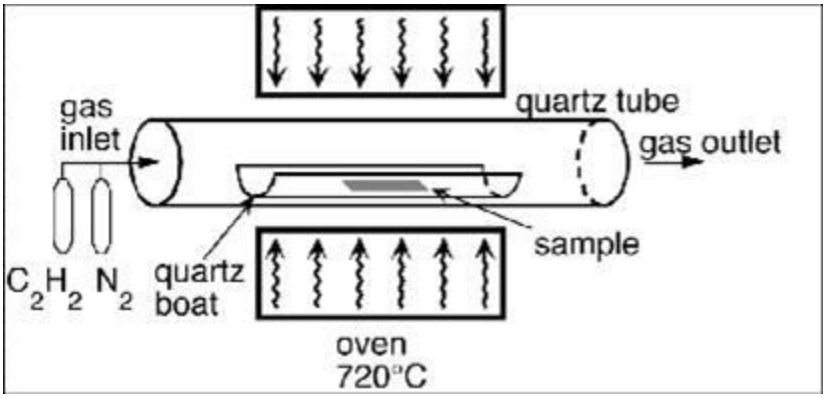

Figure 10: Chemical vapor deposition set up

1.9. Dyes:

Dyes are typically also known as pigments which are used for coloring procedure in textile and leather. These have great affinity for some specific materials and are aromatic organic compounds in nature. Dyes are mostly used in aqueous forms and the auxochrome in dyes intensify colors and increase their solubility in water. Chromophore is responsible for the color and dyes show absorption of light in visible region. They possess resonance of electrons.

1.9.1. Types of Dyes:

Dyes are classified into 2 main types:

a) Natural Dyes
b) Synthetic Dyes

Natural dyes are produced by plants and animals. Madder is an example of natural dye extracted from madder roots while cochineal is extracted from cochineal insect.

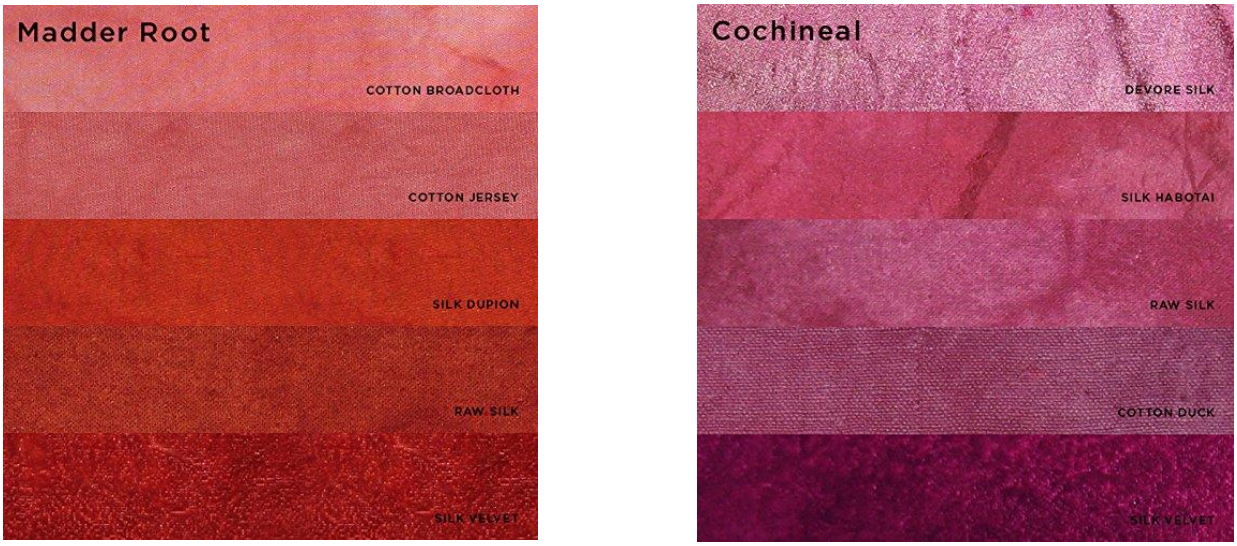

Figure 11: Madder and cochineal natural dye

Synthetic dyes are further classified into azo and non-azo dye. Azo dyes are further classified into acidic, sulfur basic reactive and dispersive dyes. Synthetic dyes are further classified on their acidic and basic nature.

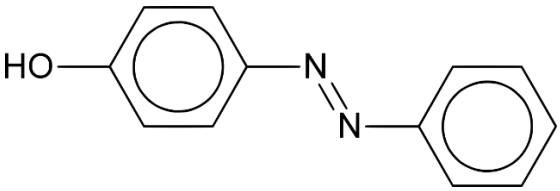

Figure12: Azo Dye

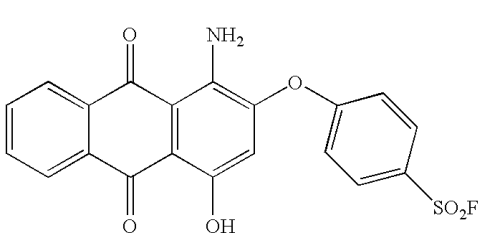

Figure: Non-azo dye

1.9.2. Need For Dye Degradation:

Dyes have benefits which are used in normal life but it has some hazards as well which are as follows:

i. Some of them are carcinogenic and some may cause irritation to skin.
ii. Dyes are soluble in water so they cause water pollution. This dye contaminated water is released in main water streams harming the human as well as aquatic life.
iii. Underwater photosynthetic activity is greatly disturbed as the reflection and absorption of sunlight is affected by these dyes [34].

So, the dyes need to be removed from contaminated water as they are lethal.

1.9.3. Methyl Orange:

It is commonly used as an indicator in titrations. It display red color in acidic while yellow color in basic media. Structure of methyl orange changes when the pH of solution changes. In case of less acidic form, this changes color from red to orange and finally yellow and vice versa in increasing acidity. Molecular structure is varied in the acidic environment because hydrogen attaches itself to nitrogen atom in N=N bond hence varying the molecular structure [35].

Figure 13: Acid and alkaline form of methyl orange

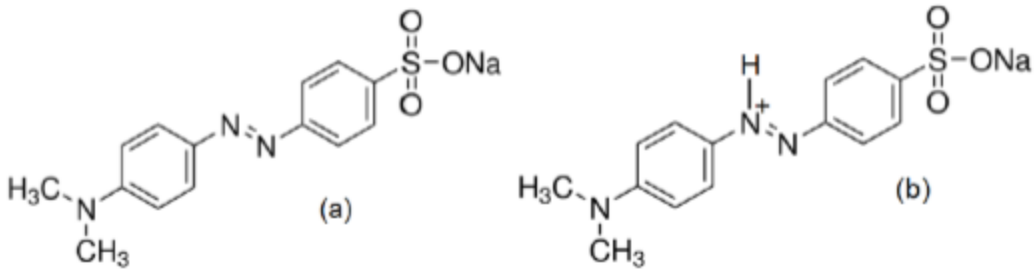

Figure 14: a) acidic form of methyl orange b) alkaline form of methyl orange

Some properties of methyl orange are as follows:

Table 1: Chemical and Physical Properties of Methyl orange

Common name	Methyl orange
IUPAC name	Sodium 4-{[4-dimethylamino] phenyl] diazenyl}benzene-1-sulfonate
Structure	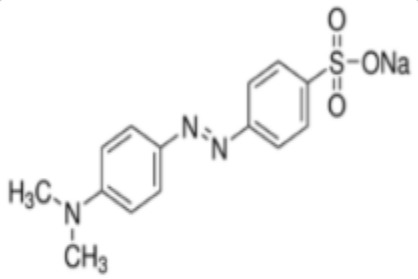
Chemical formula	$C_{14}H_{14}N_3NaO_3S$
CAS number	547-58-0
Molar mass	327.33 g/mol
Density	1.28 g/cm^3
Solubuity	Soluble in water
Metling point	>300 °C

1.10. Photocatalytic Water Splitting:

It is carried out in a photoelectrochemical cell used for the dissociation of water into its components i.e., hydrogen and oxygen in the presence of an incident source of light. Basically, only photons (light), catalyst and the water is needed [36]. Hydrogen fuel has gained fame by the increase of global warming and methods such as photocatalyic water splitting are being considered for the production of hydrogen which is also environmental friendly. Water is inexpensive renewable source [37].

The equation representing the reaction is as follows:

$$2\,H_2O \xrightleftharpoons{E > 1.23\ eV} 2\,H_2 + O_2$$

(E: photon energy.)

The minimum band gap for water splitting is considered to be 1.23ev. According to principle, the hydrogen and oxygen must occur in 2:1 stoichiometric ratio [38].

CV analysis is carried out for water splitting in which photoelectrodes are used. Photoelectrode must have a sufficient band gap for absorption of incident light which necessary to derive redox reaction of water. Metal oxides have large band gaps and produces good results. Electrode cell is used for splitting and the material is deposited as electrode by drop casting method usually. The solvent used for analysis be either KCl or KOH [39].

Electrochemical or photochemical water splitting produces electrons and protons that may combine to form hydrogen along with oxygen produced as side product. This also may combine with carbon dioxide to produce methane [40]. Therefore, photocatalysis of water is a big way to solve energy crisis and environmental issues and also produces way to use renewable form of energy and stop the use of fossil fuels which are depleting and carrying out global warming.

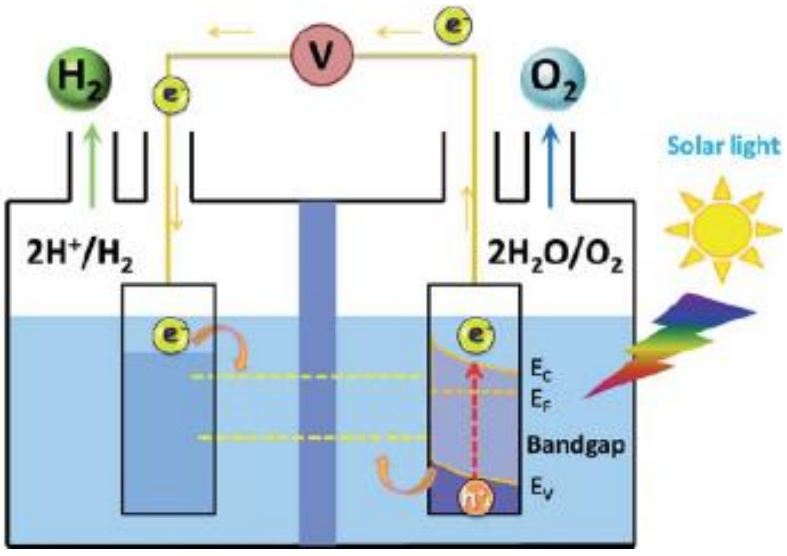

Figure 14: General representation of photochemical water splitting

1.11. Characterization Techniques:

For the analysis of optical properties, magnetic behavior, morphology, purity and crystallite size of prepared nanoparticles, characterization is carried out. Various techniques including scanning electron microscopy (SEM), X-Ray Diffraction (XRD), UV-VIS Spectrophotometry, Energy dispersive x-ray spectroscopy (EDX) etc are carried out.

1.11.1. X-Ray Diffraction (XRD):

Basic Principle:

It is used for identification of the crystalline phase of material, phase composition and structural defects.

Mechanism:

A beam of X-rays at an angle θ having a specific wavelength (λ) is made incident on the crystal to be analyzed. The incident X-rays interact with the electrons and reflect back from atomic planes of the crystal which are semitransparent so let a portion of X-Rays to pass through them and reflect the remaining rays. The incident angle θ is equal to the reflected angle and is depicted by Bragg's law.

Bragg's Law:

$2d\sin\theta = n\lambda$

And the particle size is calculated by Scherer's formula.

Scherer's Formula:

$D = K\lambda/B\cos\theta$

The incident X-Rays are focused on the surface of the crystallite. The intensity of X-rays is recorded by rotating the sample and the detector which is further attached

to a detector. Detector converts the signals and transfer them to monitor to present in data form. Goniometer in XRD machine rotates the sample and maintain the angle. Ni and Cu filters are used to retain unwanted radiation.

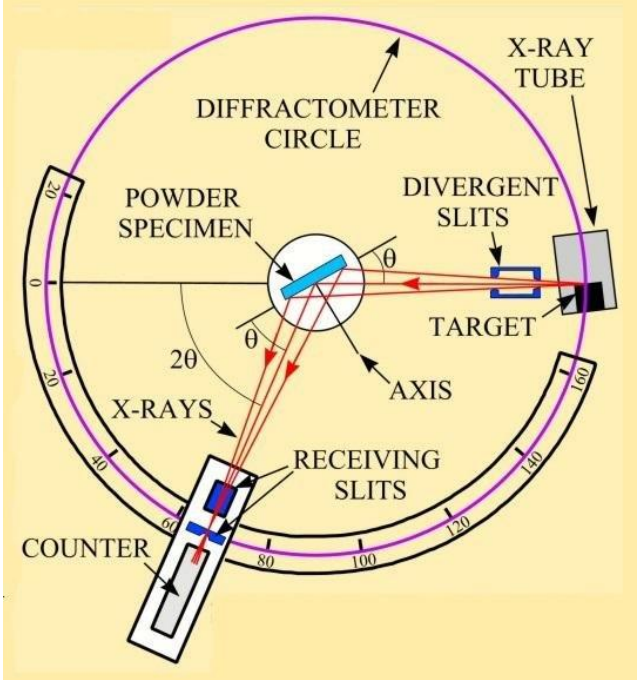

Figure 15: Schematic diagram of XRD set-up

1.11.2. Scanning Electron Microscope:

Basic Principle:

SEM produces high resolution images of the surface of compound analyzed. These images are produced in a 3-dimensional pattern by which the sample morphology is determined.

Mechanism:

A tungsten source is used which thermionically release electrons that moves in the direction of anode. Very high vacuum is retained in the system. The electron beam having energy -50 KeV is directed by single or double condenser lenses. 3 types of image are created comprising secondary electron images, back scattered electron

images and elemental X-Ray maps. Electrons having energy less than 50eV are secondary electrons which are formed from the few nm of surface of the sample and hence reveal details about the sample.

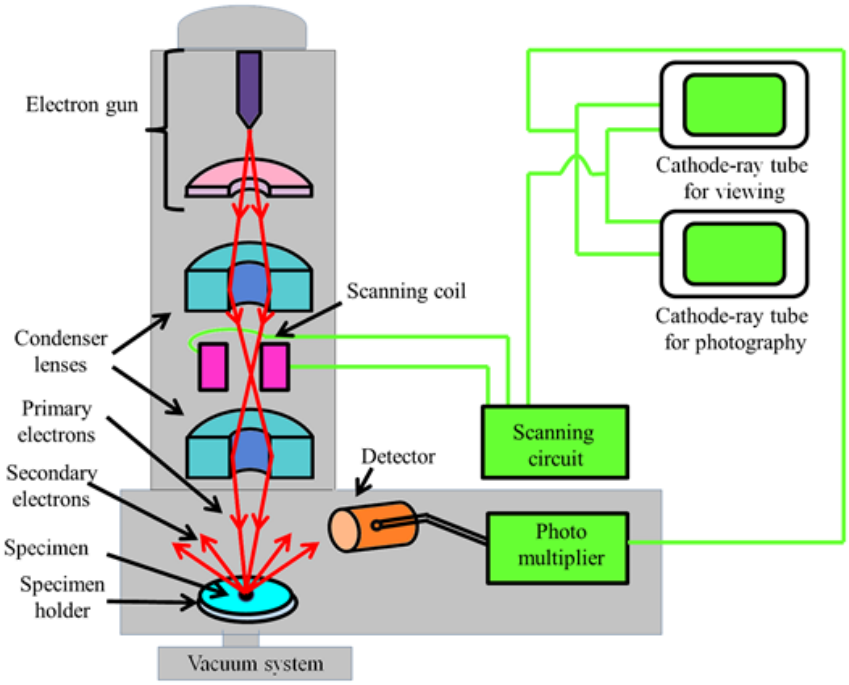

Figure 16: Schematic diagram of SEM

1.11.3. Energy Dispersive X-Ray Spectroscopy (EDX):

Basic Principle:

It revolves around the principle that every element has a distinctive atomic structure where X-rays are representative of atomic structure of that element for identification.

Mechanism:

Excitation of inner shell of electrons occur when beam of light falls on an element and a hole is created in inner shell. Therefore, an electron from outer shell transfers to inner shell to the hole to fill the vacancy. This difference of energy between the inner and outer shells carry out release of X-rays. The energy and the number of X-Rays are detected by EDS. Energy of X-rays for every element is different which permits the measurement of elemental composition of the element.

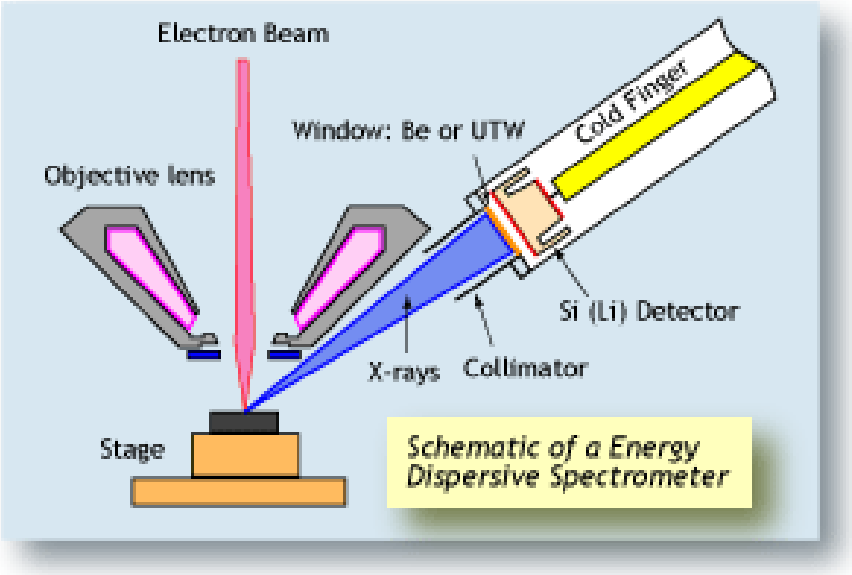

Figure 17: Schematic diagram of EDX

1.11.4. UV-VIS Absorption Spectroscopy:

Basic Principle:

Absorption of the photons is carried out with the excitation and de-excitation of electrons among different energy levels including the ground state and the excited state.

Mechanism:

Sample absorption with respect to frequency of light is evaluated by absorption spectrum. The characteristic lines of the atoms are very sharp. These spectral lines help in the determination of photon wavelength.

These spectral lines are representing some atom or ion. The fundamental gap is the difference of energy between HOMO and LUMO. It is highly efficient for characterization of nanoparticles.

UV-VIS absorption spectra range from 200 to 800nm. A good monochromator of good resolving power is employed. Deuterium lamp is used as an incident light passing through filter and then incident via inclining through a concave mirror.

Partial reflecting mirror splits the beam into two routes. One beam passes through the reference and other through the sample to be characterized.

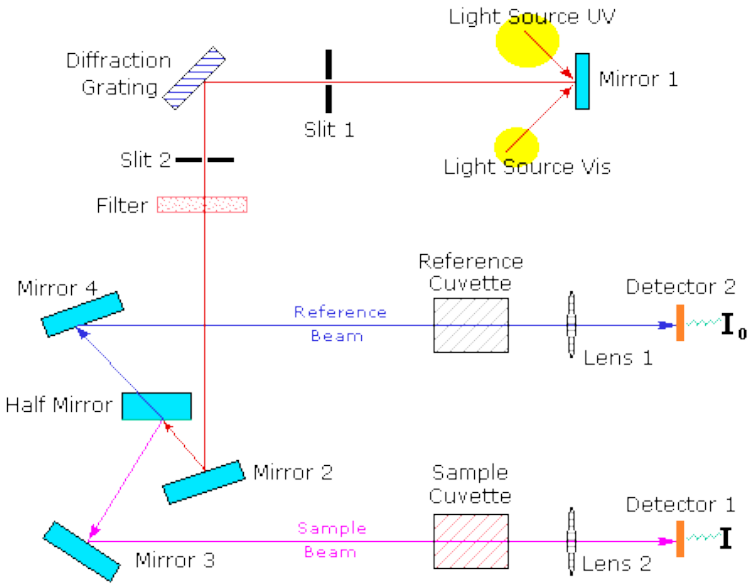

Figure 18: schematic diagram of UV-VIS spectrophotometer

Chapter 2: Literature Review

The chapter comprises of all the literature that was studied and analyzed during this research work related to nanocomposites and their applications in various fields particularly in dye degradation and water splitting. The literature comprises study work related to $NiFe_2O_4$ ad g-C_3N_4 along with ZnO added to create ternary composite and then different ratio composites formed and their activity analyzed in degradation of dyes and water splitting.

2.1. $NiFe_2O_4$ as photocatalyst

Tianyou Peng *et al.*, (2012) carried out synthesis of magnetic $NiFe_2O_4$ via hydrothermal and calcination process. The $NiFe_2O_4$ had an average diameter of 17.8nm and specific surface area of 76.2 m^2g^{-1}. It is used as a photocatalyst for hydrogen production and has visible light driven photoactivity. Therefore, it is used as an efficient catalyst in visible light driven photocatalytic reactions [41].

Hyun kim *et al.*, (2014) worked on the magnetic and photocatalytic modifications of a semiconductor material to enhance photocatalytic separation and hydrogen production by water splitting. $NiFe_2O_4$ was preferred in the process due to good photocatalytic properties and its nutshell composite was formed by binding it with TiO_2. Remarkable photocatalytic activity was observed by the combination with $NiFe_2O_4$ and hydrothermal synthesis was carried out for its preparation. It has the ability to give remarkable results of water splitting [42].

H.Y. Zhu *et al.*, (2015) used hydrothermal process to prepare to spinel nickel ferrite multi walled carbon nanotubes. They were characterized via XRD, SEM, EDS and DRS was also carried out. Photocatalytic activity was determined by degradation of congo red dye in aqueous solution under solar light irradiation. High absorption capacity could be seen towards congo red with a constant rate of 0.01433 min^{-1} which was 2.8 times that of only powdered nickel ferrite. Therefore, this can be used as a good solution for the treatment of dye contaminated waste water [13].

J.L. Arvizu *et al.*, (2017) proposed the synthesis of nanoparticles of nickel ferrite which were synthesized by Pechini's method and their optical, morphological and structural characterization was carried out by XRD, SEM, BET, and UV/VIS Spectrophotometry. Optical properties were determined by preparation of aqueous suspensions of $NiFe_2O_4$ nanoparticles in different concentration solutions. Gas chromatography was used for the determination of photocatalytic activity of $NiFe_2O_4$ for hydrogen production, thus finding a greater hydrogen production with $NiFe_2O_4$ than TiO_2 [43].

2.2. g-C_3N_4 as a photocatalyst:

Jiuqing Wen *et al.*, (2017) referred to the applications of heterogeneous photocatalysis in environmental pollution and how they are used to harvest the environmental friendly renewable solar energy sources. Various redox reactions have been derived due to various electrical, optical, and physiochemical properties in which g-C_3N_4 is widely used. Various properties of g-C_3N_4 have been described including the electrical, optical, the physiochemical properties including the crystal structure, and the surface morphology. Many applications are being followed such as water splitting to produce hydrogen, pollutant degradation, carbondioxide reduction and disinfection. By having the correct knowledge about g-C_3N_4 and its properties, it can be consumed in various applications like super capacitors, fuel cells, separation and purification and many others [44].

Amen Nasiri *et al.*, (2017) described the structure of g-C_3N_4 as a metal free conjugated polymer with a band gap of 2.7ev making it an effective photocatalyst for hydrogen production. Working of g-C_3N_4 was checked by photochemical and photoelectrochemical methods for economical production of hydrogen. Various methods have been adopted for commercial production of hydrogen employing g-C_3N_4. Different scenarios were derived for the production of ydrogen by looking at the properties and stances of g-C_3N_4 to be used as a photocatalyst [45].

Santosh Kumar *et al.*, (2018) focused on properties of g-C_3N_4 as solar fuel production through carbondioxide production and water splitting and even for environmental remediation through degradation of organic pollutants. This is due to the remarkable photophysical properties of g-C_3N_4 as well as the surface morphology charge transfer and functionalities. Hetrocomposites of g-C_3N_4 have also been

discussed in the research which enhance solar energy conversion into useable renewable energy and other applications in an efficient manner [46].

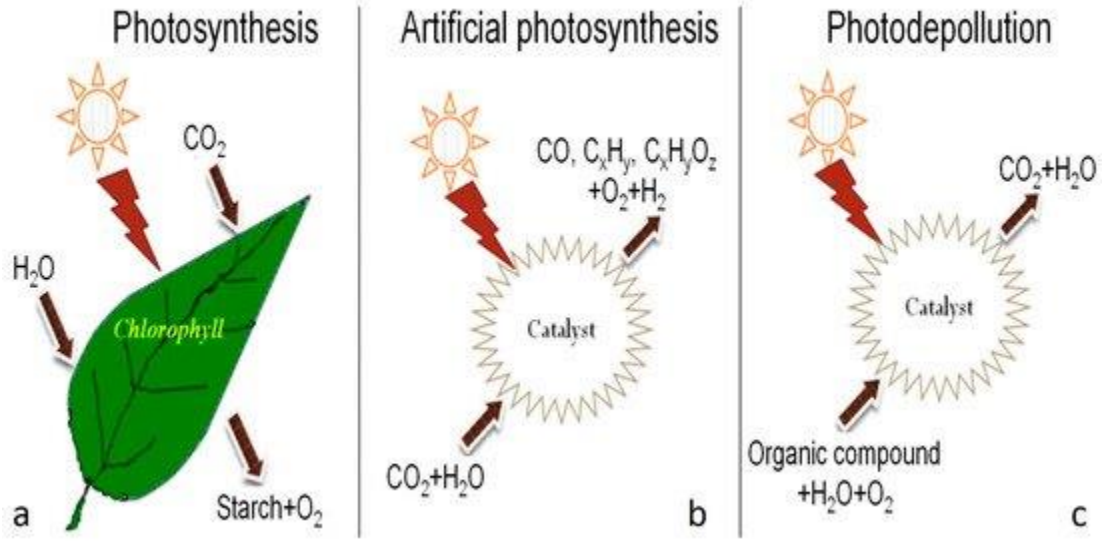

Figure 19: a) natural photosynthesis b) artificial photosynthesis through CO_2 reduction and water splitting c) photodegradation of organic pollutants in water

Chi Zhang *et al.*, (2019) has worked on the study of properties of g-C_3N_4 for degradation of pollutants as g-C_3N_4 is a two dimensional conjugated polymer used for disinfection of water, environmental remediation and solar energy conversion. Photocatalytic degradation by g-C_3N_4 for water splitting, hydrogen production, different redox reactions and water disinfection are still known. Firstly, the design and manufacture of g-C_3N_4 has been discussed and then its applications in water disinfection are being followed [24].

2.3. ZnO as a Photocatalyst:

Qiuping Zhang *et al.*, (2018) discussed the vacuum drying process for the production of ZnO powder. The oxygen vacancies are increased on the surface and the size of nanoparticles is reduced. They have discussed the role of ZnO as a photocatalyst for the decomposition of methlyne blue dye in water under UV

radiation. The catalytic activity of the catalyst remains stable throughout every cycle of degradation and efficiency exceeds up to 99% after 50 min. The photocatalytic activity and oxygen vacancies both are higher for smaller NPs. Oxygen vacancies capture electrons and small NPs have large surface areand hence better efficiency [47].

Chin Boon *et al.*, (2018) discussed about the solar photocatalysis used for the removal of organic pollutants as an environmental friendly technique. ZnO can absorb up to large portion of solar spectrum hence they are used efficiently and even cost effective for the degradation of pollutants in water. ZnO nanostructured fabrication methods are also been discussed including doping and hetrojunction with other compounds to form composites. Also the future challenges and prospects are being discussed [48].

Ghaida H. Munshi *et al.*, (2018) stated the use of green chemistry because environmental catalytic processes are in demand. Chlorophyll is a natural catalyst which is an electron rich reducing agent. The effect of spinach on preparation of ZnO was seen and photocatalytic degradation of methyl orange was seen in presence of light. Different parameters of catalytic preparation process and characterizations such as SEM, XRD and EDX were used to determine the photocatalytic activity of decomposition of methyl orange [49].

2.4. $NiFe_2O_4$ and g-C_3N_4 nanocomposite as a Photocatalyst:

Tang Linghua *et al.*, (2015) prepared the $NiFe_2O_4$/g-C_3N_4 composite in the ratio 99:1 and 90:10 by compositing nano $NiFe_2O_4$ and g-C_3N_4. The nano $NiFe_2O_4$ was added to an ethanol solution for ultrasonic dispersion and the adding g-C_3N_4 to it. The mixing is carried out in ultrasonic dispersion, then drying and converting to powder in motar and pestle and finally roasting to form the composite of $NiFe_2O_4$/g-C_3N_4. The prepared composite shows excellent photocatalytic activity and carries out efficient thermal decomposition of ammonium perchlorate so applications of both the raw materials widened after formation of composite. The preparation process is simple and economical, less preparation time and high preparation efficiency are the features of the process [50].

Haiyan Ji *et al.*, (2015) used the chemisorption method for the synthesis of $NiFe_2O_4$/g-C_3N_4 and different characterization techniques were used to analyze the properties and structure of the sample which showed that the $NiFe_2O_4$ was integrated onto g-C_3N_4. The prepared 7.5% $NiFe_2O_4$/g-C_3N_4 composite maintain high photocatalytic activity and efficiency in visible light irradiation. Photo-Fenton process is carried for charge separation between $NiFe_2O_4$ and g-C_3N_4 to get an enhanced photocatalytic activity [28].

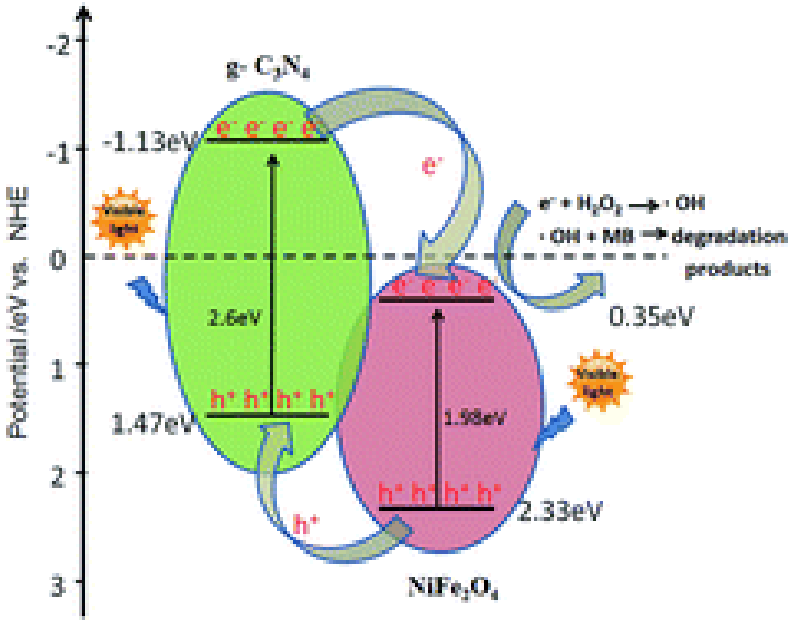

Figure 20: band gap diagram of $NiFe_2O_4$ and g-C_3N_4

Yong Liu *et al.*, 2018 discussed about the spinel structure of nickel ferrite which was doped with g-C_3N_4 by the help of coprecipitation method to form the composite $NiFe_2O_4$/g-C_3N_4 and then used in the photocatalytic activity for the degradation of methyl orange. In comparison to pure $NiFe_2O_4$ and pure g-C_3N_4 the composite of $NiFe_2O_4$/g-C_3N_4 has much more efficiency. This composite of $NiFe_2O_4$/g-C_3N_4 inhibit the recombination of photo excited electron-hole pairs, enhance visible light absorption and charge separation [36].

Gebrehiwot Gebreslassie *et al.*, (2019) referred to the synthesis of $NiFe_2O_4$/g-C_3N_4 by the help of one-pot hydrothermal synthesis. The characterization techniques used were XRD, FTIR, SEM, EDS, BET and TEM which helps in visual representation of $NiFe_2O_4$ nanoparticles on g-C_3N_4 sheets. The photocatalytic activity for degradation of methyl orange was checked and it was seen that the photocatalytic activity of $NiFe_2O_4$/g-C_3N_4 was 4 times higher than the pristine $NiFe_2O_4$ and g-C_3N_4 remains in Z-scheme providing efficient space for separation of charge carrier. This Z-scheme provides efficient method for removal of contaminants from water [37].

2.5. $NiFe_2O_4$/g-C_3N_4/ZnO hetro-composite as a photocatalyst:

Yunjin Yao *et al.*, (2014) proposed the preparation of $ZnFe_2O_4$/g-C_3N_4 hybrid which were successfully synthesized by reflux treatment of $ZnFe_2O_4$ with g-C_3N_4 sheets in methanol at 90°C. The characterization is carried out by SEM, XRD, EDS and high resolution TEM. UV-VIS Spectroscopy was used for the discoloration of methyl orange. The characterizations revealed the remarkable photocatalytic activity of $ZnFe_2O_4$/g-C_3N_4 over the traditional Fenton system. The composite $ZnFe_2O_4$/g-C_3N_4 was quite stable and the stability continued even after five runs showing the high efficiency of the composite in photo degradation of organic pollutants [51].

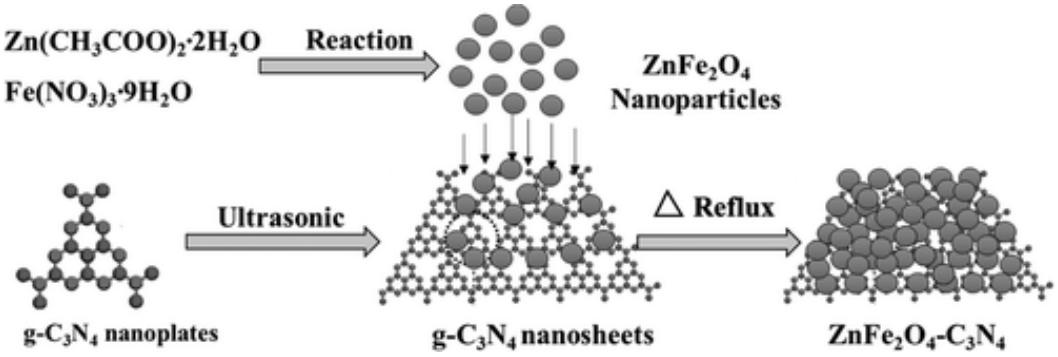

Figure 21: schematic illustration of preparation of composite $ZnFe_2O_4$/g-C_3N_4

Jinze Li *et al.*, (2015) discussed the composite formation of g-C_3N_4/ZnO/HNT which are halloysite nanotubes for the formation of nanocomposite photocatalyst via facile calcination method to enhance the visible light photocatalytic activity of the composite and the stability and activity of ZnO for degradation of organic pollutants. The proposed the combination of different metallic compounds to ZnO and g-C_3N_4 such as $NiFe_2O_4$ and $CoFe_2O_4$ to increase the surface area of g-C_3N_4 for efficient

charge transfer and photoexcited charge carriers. The charge transfer and separation rate of electron-hole pair generated was determined by electron spin resonance (ESR) spin-trap technique [52].

Dionysios *et al.*, (2016) generally referred to the degradation of organic pollutants via the help of ZnO and graphitic compounds with a blend of metallic compound. It provides information about the environmental friendly methods and compounds formed for the degradation of contaminants in water. One of the case he presented was of g-C_3N_4 and ZnO with different metallic compounds such as those of Nickle and Iron. However, these nanocomposites are formed in powdered form and are used as photocatalysts to eliminate secondary pollution. The role of composite was not just discussed in pollutants degradation but also the photoelectrical properties such as those discussed in water splitting to generate hydrogen was also discussed [53].

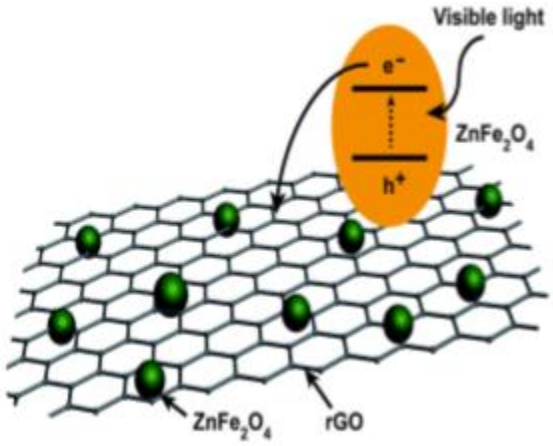

Figure 22: charge transfer in RGO/$ZnFe_2O_4$

Chapter 3: Experimental Work

This chapter comprises details of experimental work including preparation of target materials and their characterization.

3.1. Synthesis of $NiFe_2O_4$ Nanoparticles:

Hydrothermal synthesis was used for the preparation of $NiFe_2O_4$ nanoparticles. The salts of $Fe(NO_3)_3.9H_2O$ and $Ni(NO_3)_2$ were employed as precursors in the process. Polyethylene glycol (PEG) was used as a surfactant.

3.1.1. Procedure for Synthesis of $NiFe_2O_4$ Nanoparticles:

Both precursor salts were used in solution form. 25ml solutions of 0.4M $Fe(NO_3)_3.9H_2O$ and 0.2M $Ni(NO_3)_2$ were prepared in distill water. Subsequently both solutions were poured into a conical flask with stirring to mix them together. Small amount 0.2g of Polyethylene glycol (PEG) was added to control the morphology of nanoparticle. An alkaline solution of 1.5M NaOH was prepared for precipitation of $NiFe_2O_4$ nanoparticles. This basic solution was slowly added dropwise into the precursor solution under rigorous stirring while the pH was monitored consistently during the process and maintained between 7 to 8.

Resultant suspension flask was placed on a hot plate and heated up to 80^oC under continuous stirring for one hour. Afterward, suspension was cooled down to room temperature for centrifugation to retrieve the product. Centrifugation was carried out for 15-20 minutes at 3000rpm which furnished black precipitates of the product. Resultant product was separated and washed with ethanol and distilled water thrice to remove the surfactant. The product was then dried at 80^0C in a drying oven for 9-10 hours to completely remove the moisture. Dried nickel ferrite solid was obtained which was further crushed and grounded to be converted into powder form. In case, if any residual moisture was observed due to incomplete drying, then another heating cycle was carried out in drying oven at 50^oC for further 5 hours.

+

$Ni(NO_3)_2$ solution

$Fe(NO_3)_3.9H_2O$ Solution

$Ni(NO_3)_2$ + $Fe(NO_3)_3.9H_2O$ Solution

NaOH slowly added to conical flask having both salt solutions + pH monitored

pH6-7 maintained

stirring carried out with heating on hot plate

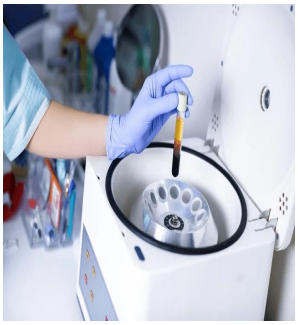

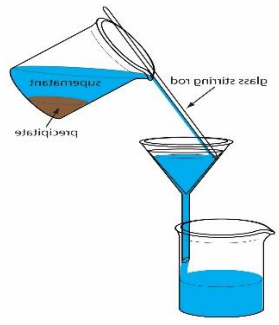

Centrifugation to

washing of precipitates

Drying of ppt

separate ppt

Crushed $NiFe_2O_4$

Obtained

Figure 23: Flow diagram for the synthesis of $NiFe_2O_4$ nanoparticles

3.2. Synthesis of g-C_3N_4:

Preparation of graphitic carbon nitride was carried out by melamine which is the exclusive chemical for preparation of g-C_3N_4.

3.2.1. Procedure for synthesis of g-C_3N_4:

About 2g of melamine white powder was weighed at the weighing machine and put in a ceramic crucible. Ceramic crucible was used so that it can bear the high temperature of calcination furnace. The temperature of the calcination furnace was set at 550^{o}C at the rate of 5^{o}C per minute and the melamine in covered ceramic crucible was placed in it for almost 3 hours. After the reaction was completed, yellow colored solid of melamine was obtained. It was allowed to cool and crushed into powdered form.

Melamine in crucible | calcination carried out in calcination furnace | g-C_3N_4 powder

Figure 24: Flow diagram for synthesis of g-C_3N_4

3.3. Synthesis of ZnO:

Zinc nitrate as a precursor and KOH as a strong base was used in the process.

3.3.1. Procedure for the synthesis of ZnO:

0.2M aqueous solution of zinc nitrate and 0.4M solution of KOH was prepared in distilled water separately. The KOH solution was added to ZnO solution slowly with vigorous stirring to maintain the pH by 10 which was continuously checked by pH meter. White precipitates of ZnO were formed by addition of KOH. The white product was then centrifuged at 5000rpm for 5 to 20 minutes to separate the product. The product was separated and washed thrice with alcohol and distilled water. The product was then calcined at 500^{o}C for 3 hours.

$ZnNO_3$ solution KOH solution white ppt formed by addition of KOH to ZnO solution

Centrifugation of ppt washing of ppt Drying of ppt

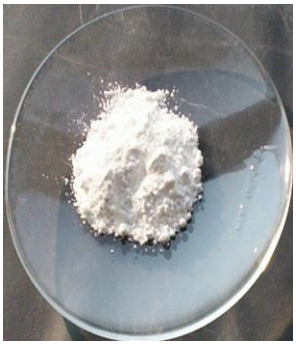

Solid ZnO powdered ZnO

Figure 25: Flow diagram for synthesis of ZnO

3.4. Preparation of $NiFe_2O_4$/g-C_3N_4 nanocomposite:

Hydrothermal method and ball milling both were employed for the preparation of this composite. Both $NiFe_2O_4$ and g-C_3N_4 were added in a beaker in ethanol with vigorous stirring and heating to mix them well for one hour. Then these were placed in drying oven at 80^{o}C for 3 to 5 hours to remove all moisture. The product removed was then crushed and converted to powdered form. Different ratios of product was prepared by this method as follows:

1. nc-i was 1:1
2. nc-ii was 1:3
3. nc-iii was 3:1

Table 2: Details of $NiFe_2O_4$/ g-C_3N_4 nanocomposite

Sr. No.	**Composite Name**	**Ratio of $NiFe_2O_4$ by %**	**Ratio of g-C_3N_4 by %**
1.	nc-i	50	50
2.	nc-ii	25	75
3.	nc-iii	75	25

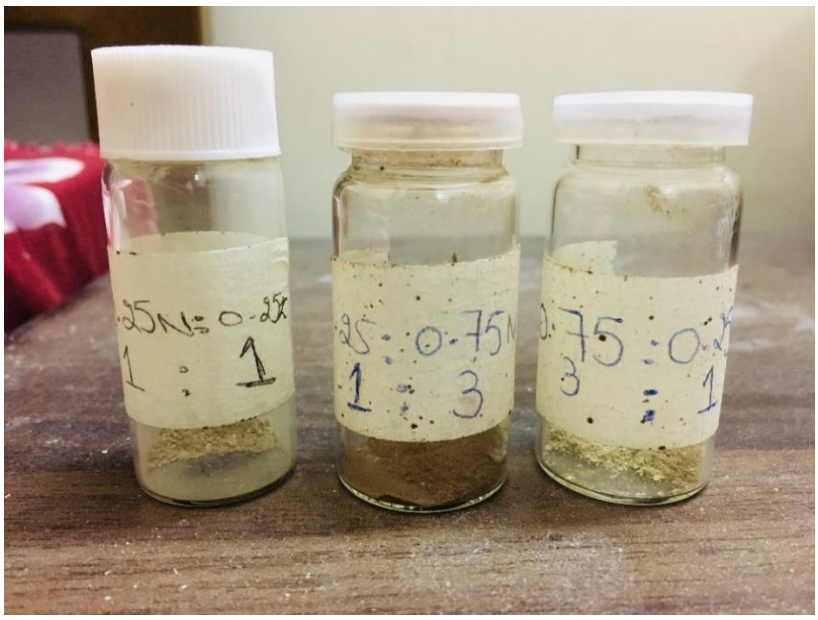

Figure 26: Ratios of composite $NiFe_2O_4$/g-C_3N_4 nc-i, nc-ii and nc-iii

3.5. Preparation of $NiFe_2O_4$/ g-C_3N_4/ZnO nanocomposite:

Above mentioned procedure was also repeated in the preparation of this nanocomposite. All the components were separately added in ethanol and stirring with heating carried out for one hour in a beaker. Then the product was dried in drying oven and was crushed and converted into powder. This powder was calcined at 500^{o}C for 3 hours. It was let down to cool and again crushed into powder form and subsequently characterized. Three ratio composites were formed by this method:

1. NC-1 was 1:1:1
2. NC-2 was 1:3:1
3. NC-3 was 3:1:1

Table 3: Details of $NiFe_2O_4$/ g-C_3N_4/ZnO nanocomposite

Sr. No.	**Name of Composite**	**Ratio of $NiFe_2O_4$ by %**	**Ratio of g-C_3N_4 by %**	**Ratio of ZnO by %**
1.	NC-1	50	50	50
2.	NC-2	25	75	25
3.	NC-3	75	25	25

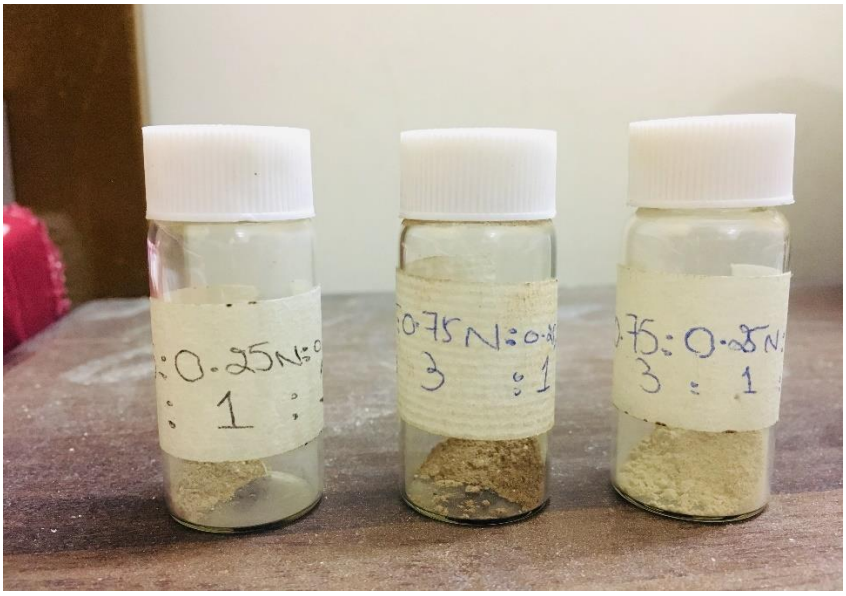

Figure 27: Ratios of composite $NiFe_2O_4$/ g-C_3N_4/ZnO NC-1, NC-2, and NC-3

3.6. Dye Degradation Experiment:

Degradation studies were carried out on methyl orange to check the photocatalytical properties of the prepared nanocomposites. Pure methyl orange was used to prepare 3ppm dye solution. Photo-reactor was used in the process with light source of 300W Xe arc lamp that was placed at a distance of 25cm from the beaker containing dye solution.

Initially, experiment was carried out with only stock solution with no catalyst added i.e., blank solution. Subsequently, 100ml of stock solution was taken in different beakers in which 10mg of each catalyst was added. These solution were then separately kept in dark and stirring was carried out for 1 hour to attain absorption-desorption equilibrium to allow maximum absorption of methyl orange on the surface of the catalyst. Samples were then kept in photo-reactor with light irradiated on it while 5ml of samples were retrieved from each irradiated solution with an interval of 30 minutes for 3 hours. These samples of 5ml each were then centrifuged for 5 minutes at 10000 rpm to let the catalyst settle down. These resultant solution samples were then analyzed by UV-VIS spectrophotometer to study the extent of dye degradation by each catalyst.

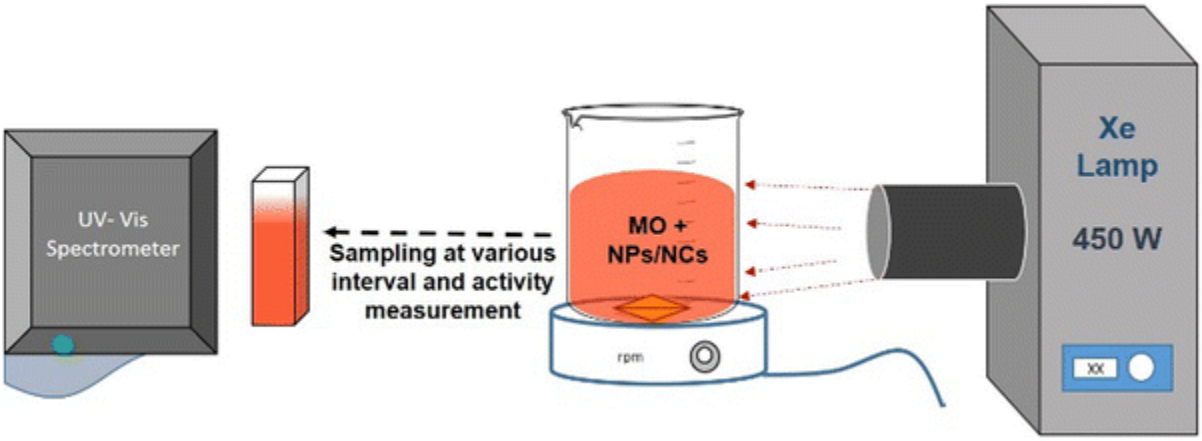

Figure 28: Dye degradation set-up of methyl orange

3.7. Water Splitting:

This involves the pre-casting of electrodes from the nanocomposites that were prepared earlier. The electrodes were prepared by addition of each catalyst in ethanol in eppendorfs and then the sonication was carried out for 15 minutes to let them mix well. The electrodes were prepared by drop casting method with the help of dropper on fluorine doped tin-oxide coated glass (FTO) which was first checked by the multimeter to determine its conductive side.

The coating was carried out on the conductive side drop wise. A single drop of different composite samples was casted on each FTO separately and was allowed to air dry. This procedure was repeated and further drops were casted to form a thick

layer on the FTO. After a thick layer of catalyst was formed on the FTO, a binder named nafion was added on each FTO and air dried so that the catalyst was bonded permanently on the FTO and did not disintegrate during the analysis. As prepared electrode was connected to the CV circuit in KCL solution and the cycle was run. The linear sweep voltammetry was scanned at different voltage ranging from 5mV to 100mV. Also, a stability cycle was run to check the stability of each catalyst to perform water splitting reaction.

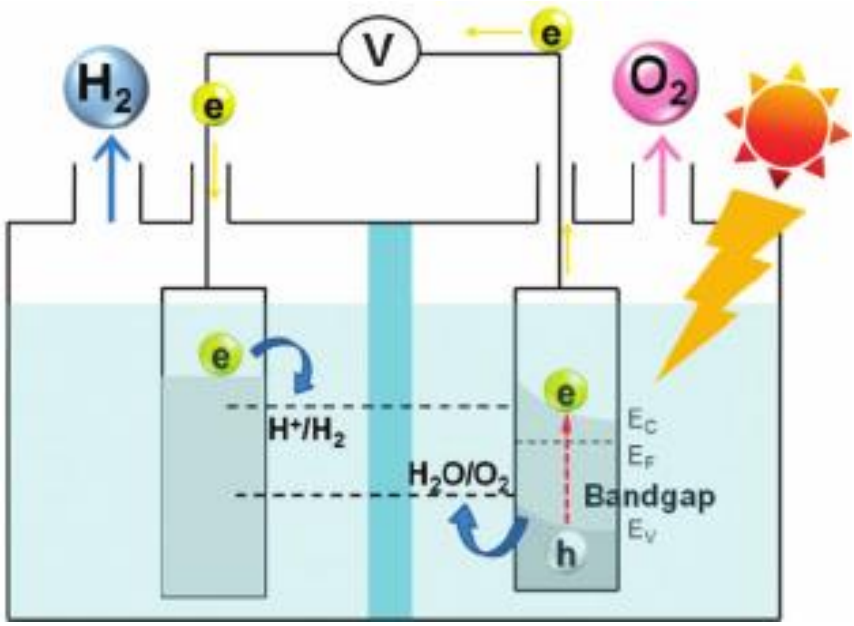

Figure 29: Water splitting via incident light radiations

Chapter 4: Results and Discussion

4.1. XRD Analysis:

The XRD patterns of all the prepared samples were obtained in the range of 10° to 70° by Cu-K_a radiation. The standard used for $NiFe_2O_4$ was JCPDS 54-0964 which shows that the strongest diffraction peak at 28.3° matching well with (111) diffraction plane. This showed the crystalline planes of $NiFe_2O_4$ and no impurity of the samples was detected. The standard used for g-C_3N_4 JCPDS 87-1526 which showed the strongest XRD peak at 27.5°C which can be indexed at (002) diffraction plane. The standard then followed for ZnO was JCPDS 36-1451 indicating hexagonal diffraction planes of ZnO and the best peaks at 28.0°C and 30.0°C. No extra peaks are present thus, indicating the purity of the sample. The three composites of $NiFe_2O_4$/g-C_3N_4/ZnO formed in different ratios showed the blend of all peaks of the pure elements. The peaks of $NiFe_2O_4$, g-C_3N_4 and ZnO can be seen in all three composites.

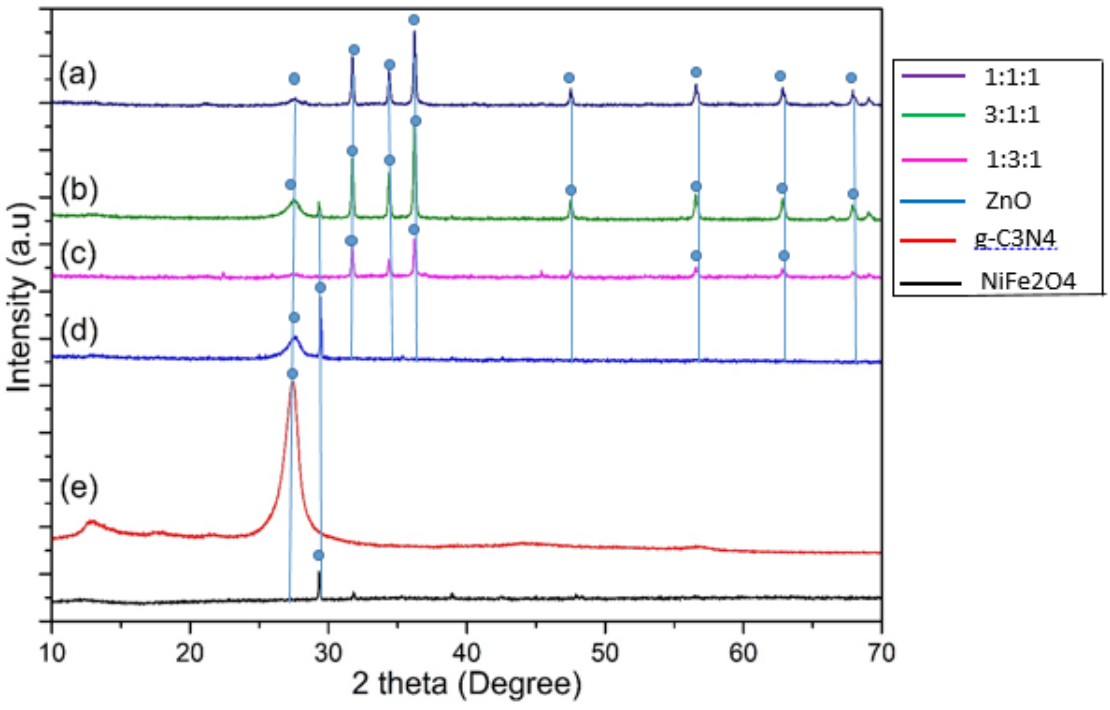

Figure 30: XRD patterns of (a) NC-1 (b) NC-2 (c) NC-3 (d) ZnO (e) g-C_3N_4 and (f) $NiFe_2O$

4.2. Scanning Electron Microscope (SEM):

SEM was carried out for morphological analysis and images were recorded at different resolutions. It can be clearly seen from the image that $NiFe_2O_4$ has 2 types of morphologies: the large polygon plates and the nanoscale particles. Therefore, it can be assumed that the crystallite size distribution of $NiFe_2O_4$ could be bimodal [54]. The nanoparticles formed were uniform which agglomerated to form rectangular plates like structure. The surface of the nanoparticles has pores which were created due to release of gases during reaction and further after drying of in oven.

The g-C_3N_4 has a wrinkle two-dimensional structure and a layered structure due to the presence of graphite hence the composite formed will also be layered. The particles are aggregated containing a large number of irregular smaller crystals. The aggregated morphology is comprised of block-based flakes and particles. These flakes on further calcination are converted into nanoparticles.

ZnO has a very organized flower shaped pattern. ZnO was calcined at 300^oC and then 500^oC which first converted it into nanoflakes and then into nanoparticles which are visible in the images given below. Therefore, we can comment that the morphologies of ZnO changes with calcination temperature. However, the agglomeration occurs among the particles with the rise in calcination temperature which is depicted as a flower shaped cluster morphology clearly evident in the high resolution SEM images.

The high resolution SEM images provides the evidence that the graphene nanosheets are well decorated by ZnO and $NiFe_2O_4$ nanoparticles, which are densely and uniformly deposited on surface of graphene to form a sandwich like structure. The image clearly shows the uniform rectangular shaped $NiFe_2O_4$ lying at the bottom with a layer of g-C_3N_4 and agglomerate of ZnO placed right on the surface of rectangular plate giving it a sandwich like morphology indicating the prepared nanocomposite.

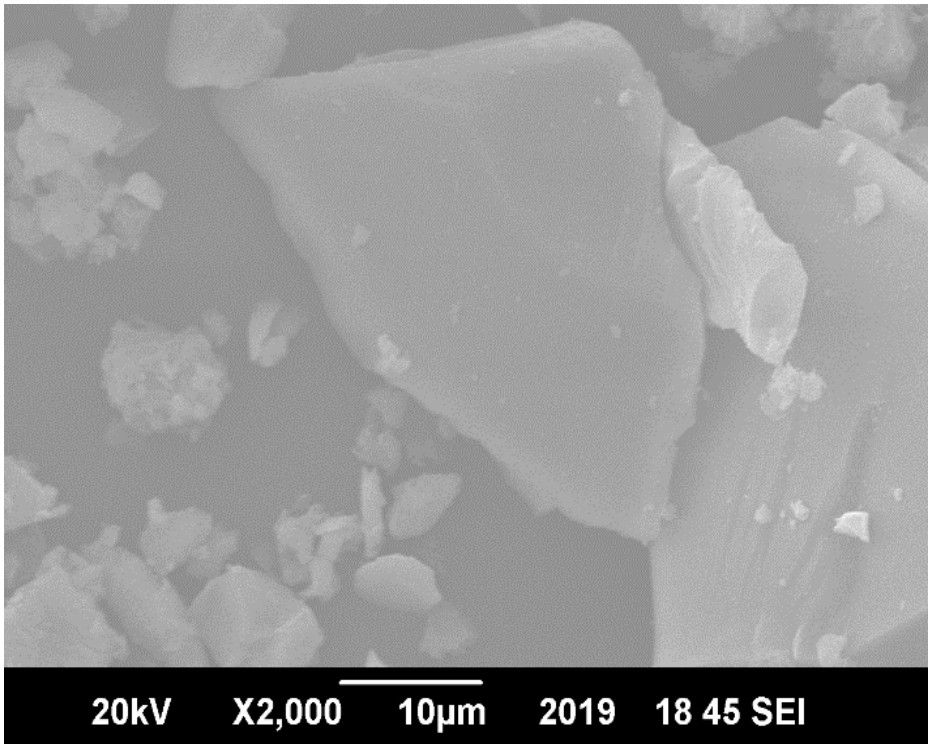

Figure 31: SEM image of $NiFe_2O_4$

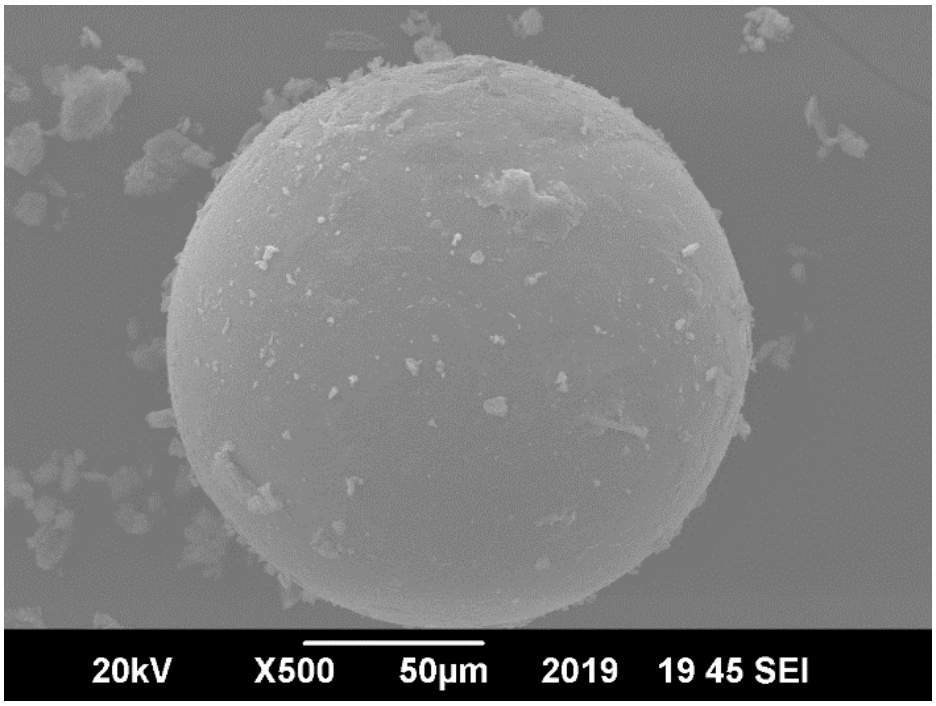

Figure 32: SEM image of single nanoparticle of $NiFe_2O_4$

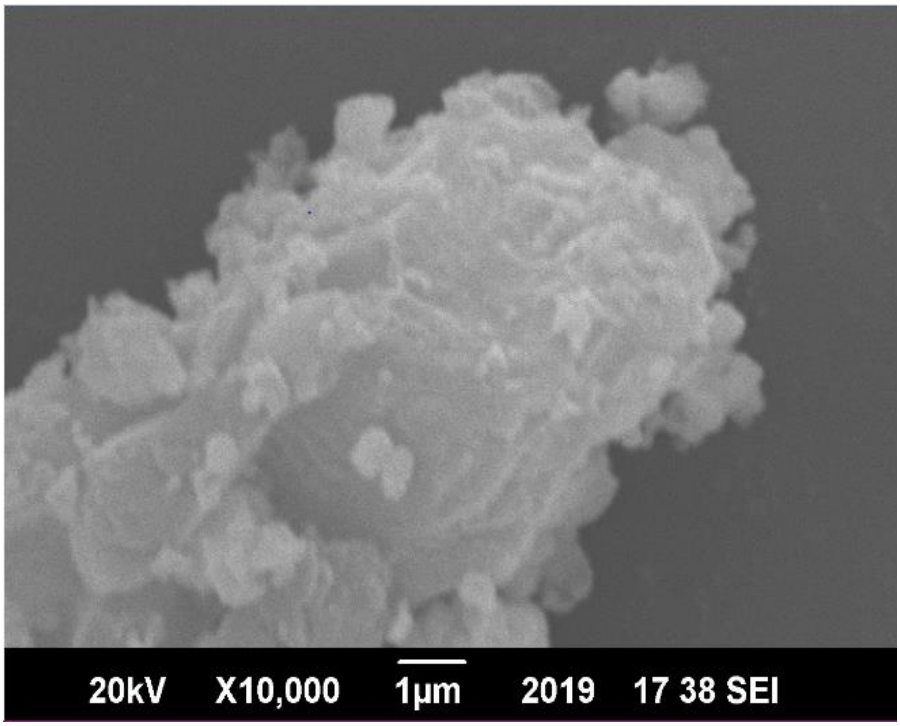

Figure 33: SEM image of g-C3N4

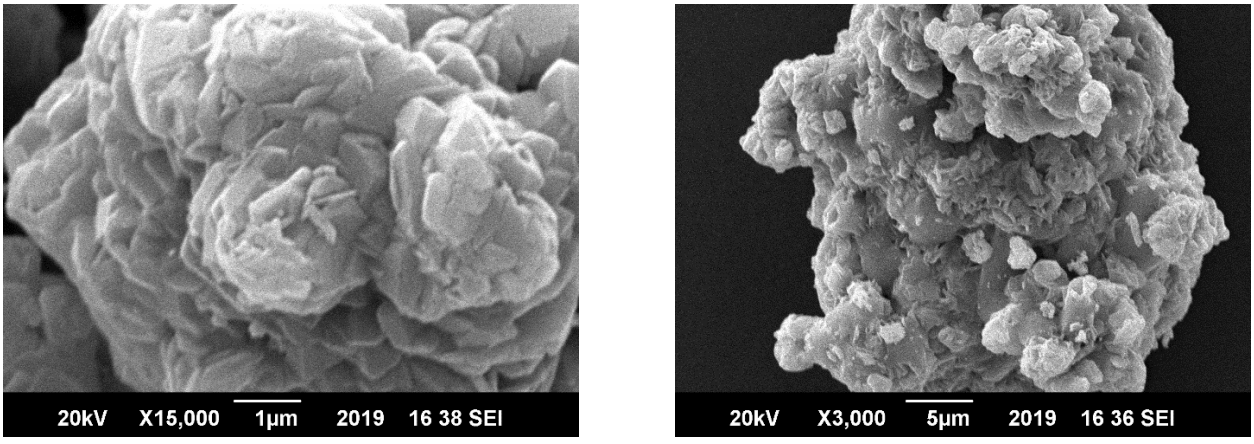

Figure 34: SEM images of ZnO

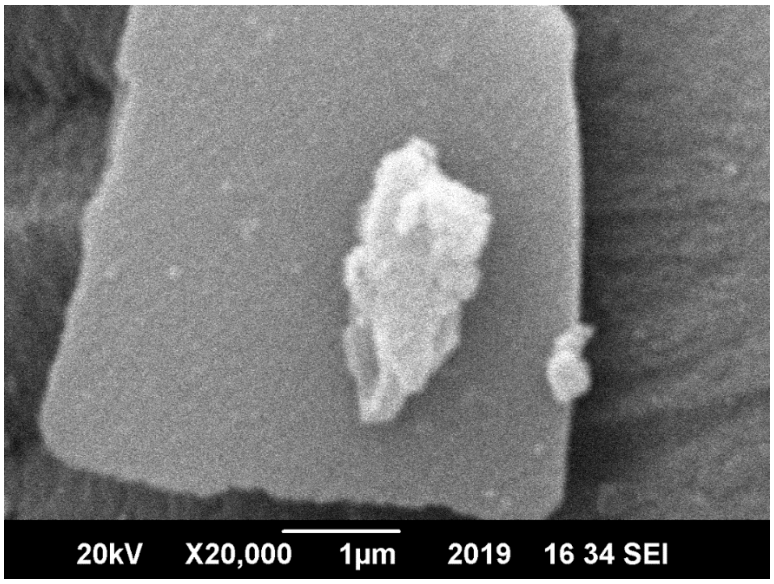

Figure 35: SEM image of NC-1 1:1:1

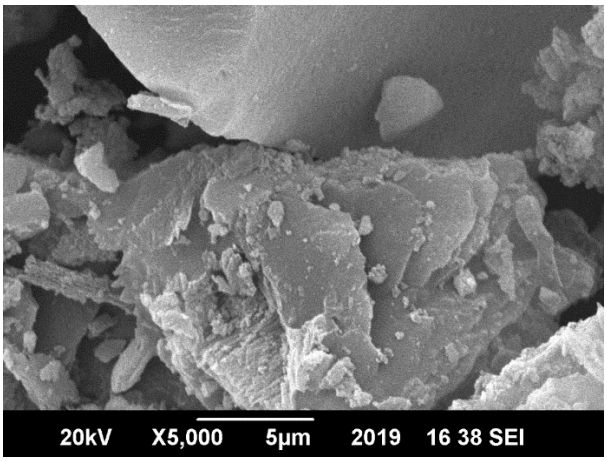

Figure 36: SEM image of NC-2 1:3:1

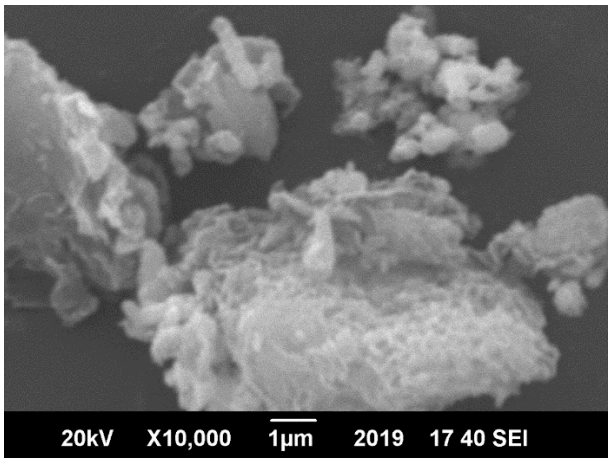

Figure 37: SEM image of NC-3 3:1:1

4.3. Diffuse Reflectance Spectroscopy (DRS) and Tauc Plots:

The tauc plots of prepared spectra were plotted by obtaining DRS spectra. Tauc plots were plotted between photon energy and $(\alpha h\nu)^2$ for the calculation of band gaps of the nano composites obtained to analyze their working in applications such as water splitting.

A comparison of the DRS analysis of all the composites is shown in the following graph.

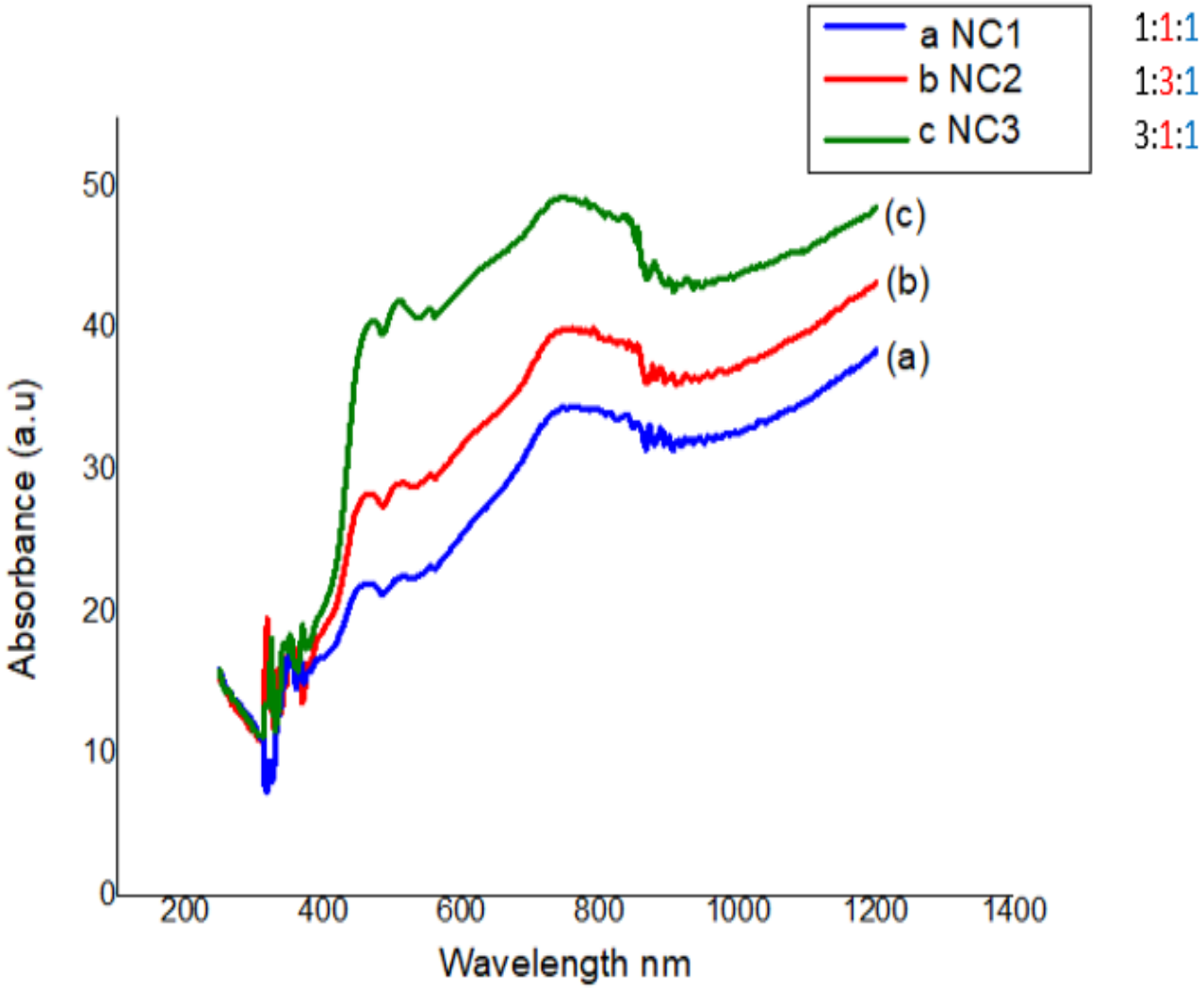

Figure 38: Comparison of DRS analysis of the 3 prepared nano catalysts

The above graph shows the least absorbance for the NC-1 (1:1:1) because it has the least band gap and highest capacity to carry out dye degradation and water splitting to produce hydrogen with highest percentage efficiency. If we look at other two composites, the band gap increases, hence the absorbance is not much effected.

Below are the tauc plots for all three prepared nano composites.

The tauc plot of NC-1 (1:1:1) shows the least band gap therefore, it capture electron and holes efficiently and gives the best activity in comparison to the other two with large band gaps.

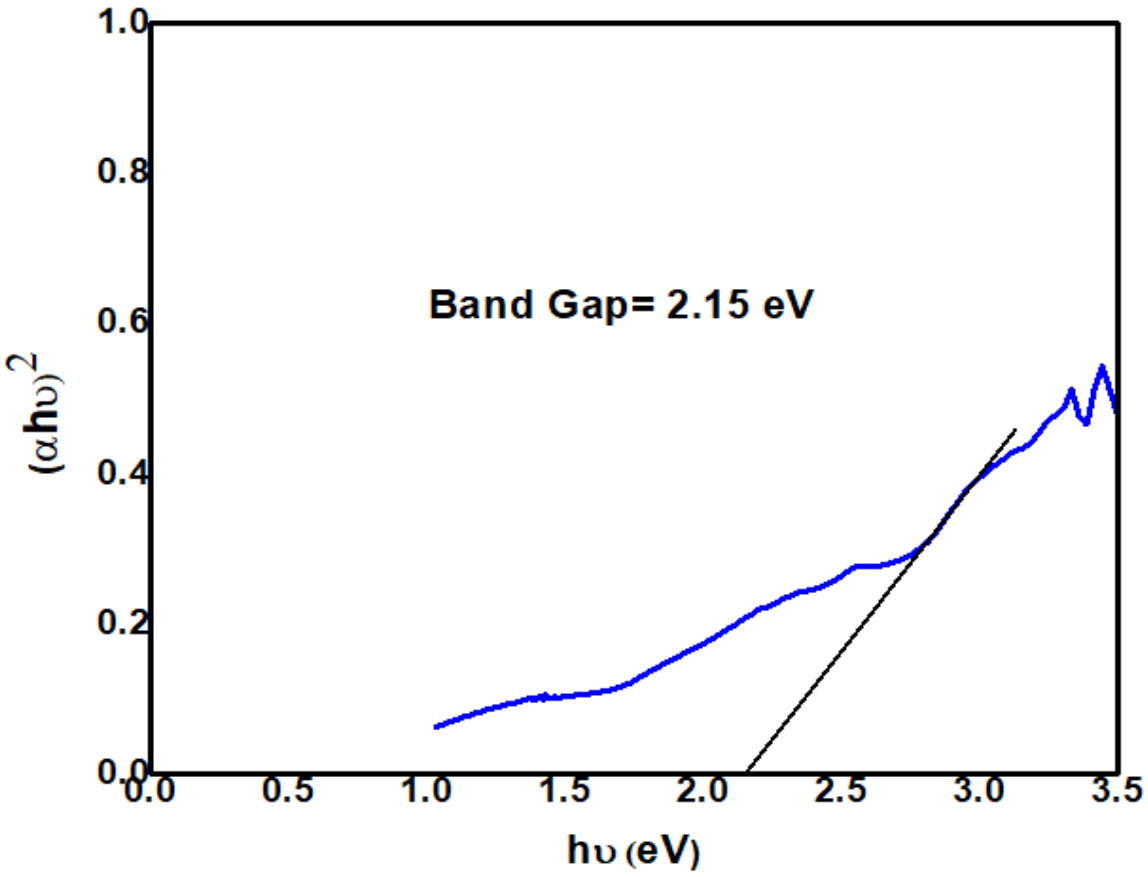

Figure 39: Tauc plot of composite 1:1:1 with band gap of 2.15Ev

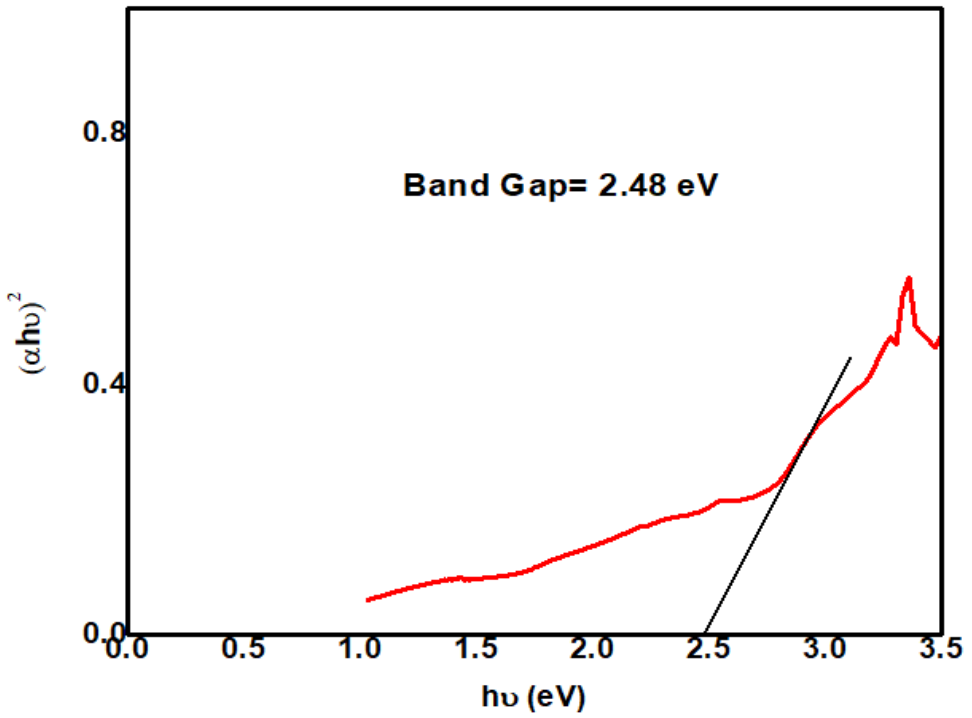

Figure 40: Tauc plot of composite 1:3:1 with band gap of 2.48Ev

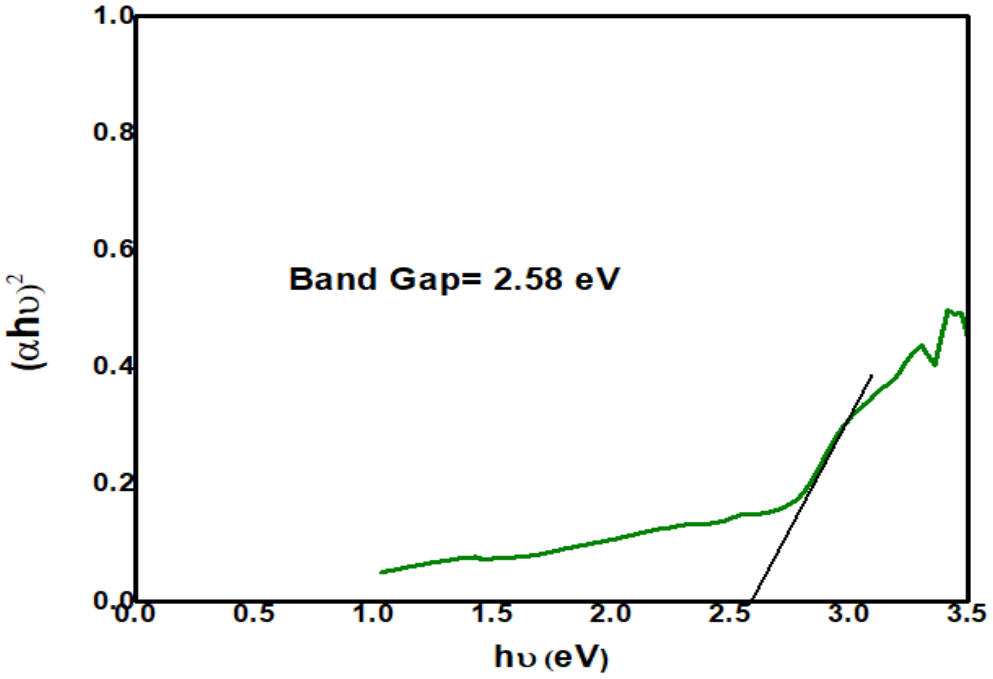

Figure 41: Tauc Plot of composite 3:1:1 with highest band gap 2.58eV

4.4. UV Analysis:

The photocatalytic activity measurement was carried out at by UV analysis which shows that the characteristic absorbance peak of methyl orange is typically at 464nm but it should decrease the absorbance at this point via dye degradation.

The best result termed out was of the composite 1:1:1. This shows almost 78% degradation % efficiency. We can see in the following graph that the dye degradation is maximum for composite 1:1:1 clearly indicated by the decrease in absorbance in UV spectrophotometer. The graph is at different time intervals ranging from blank up to 120 minutes (2hrs.). in comparison to this, if we look at the results of composite 1:3:1, it is clear that the decrease in absorbance is very low which shows almost no change in graph and the % degradation efficiency by only 30% and similarly for composite 3:1:1 where the % degradation efficiency is only 19%.

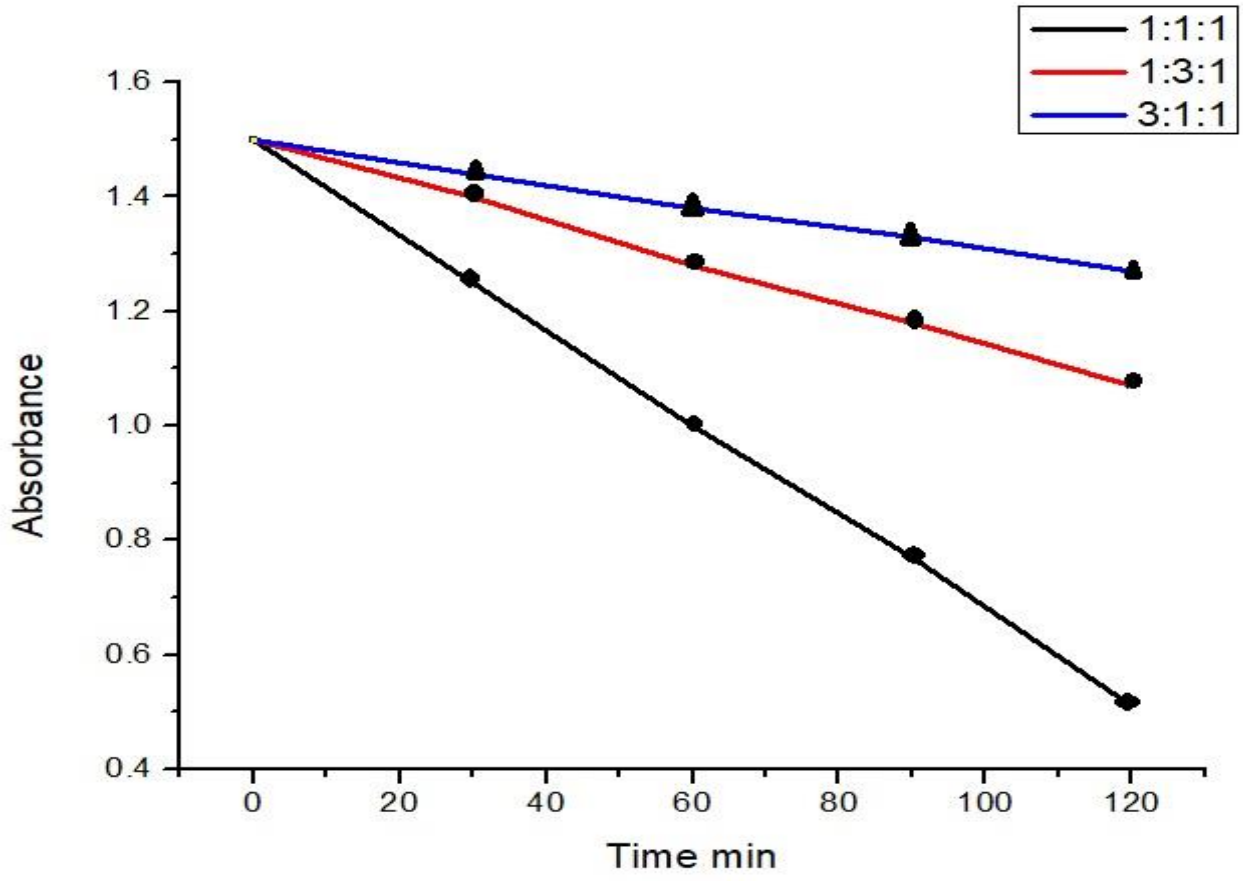

Figure 42: Dye Degradation of methyl orange in A. NC-1 B. NC-2 and C. NC-3

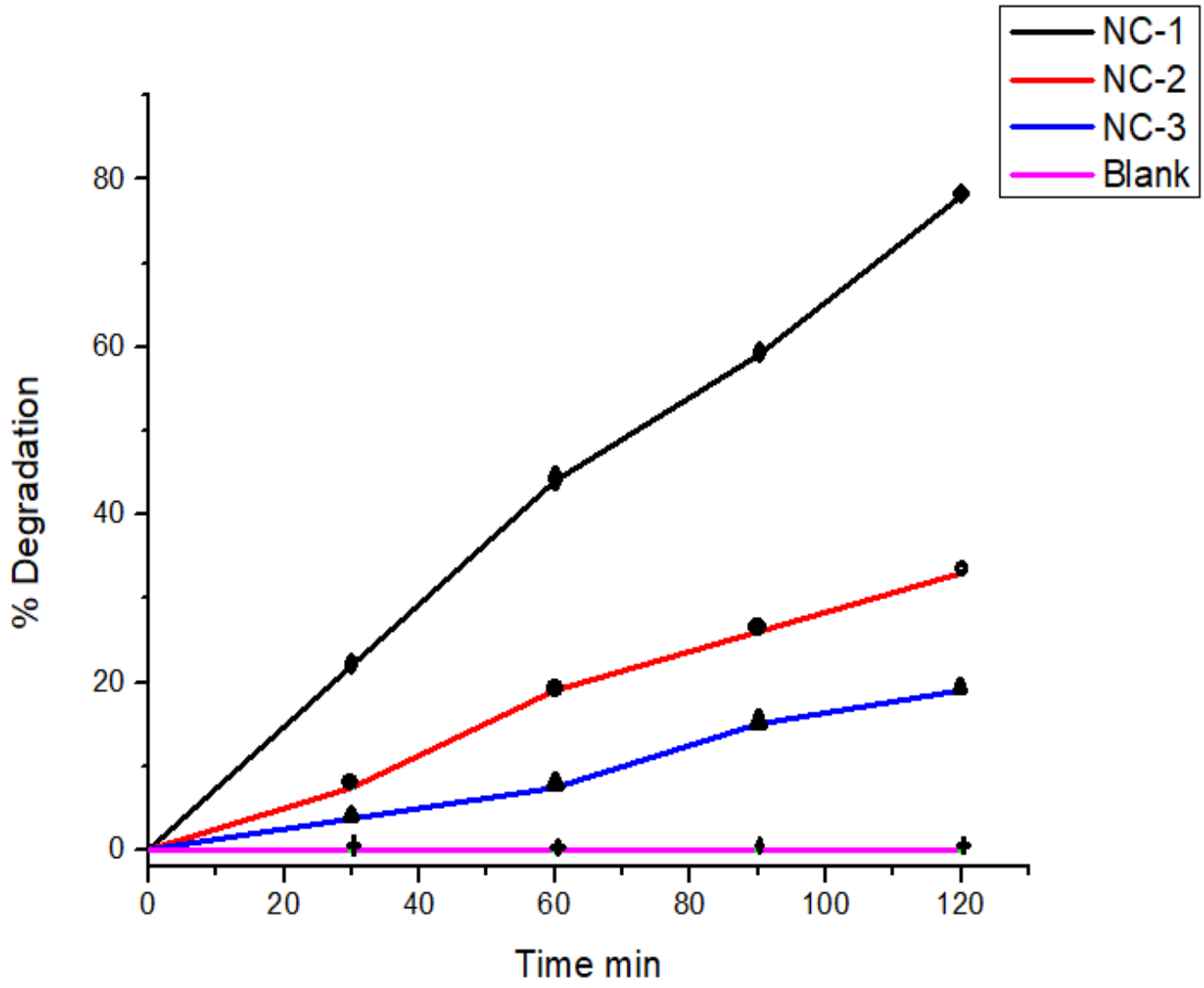

Figure 43: The % degradation of methyl orange for all prepared nano catalysts is being shown in this figure against time

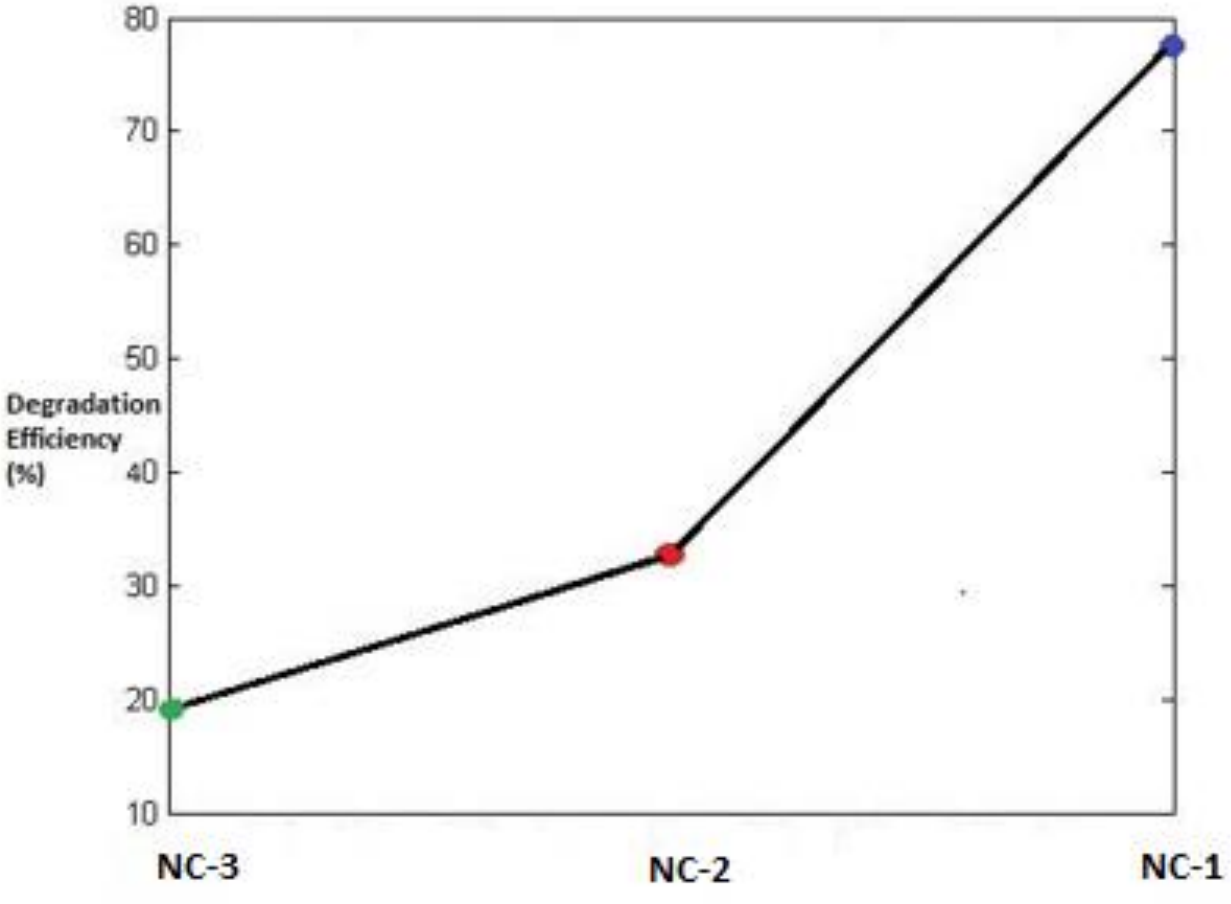

Figure 44: comparison of percentage degradation efficiency of NC-1 (3:1:1), NC-2 (1:3:1) and NC-3 (1:1:1) against methyl orange

Nano composite 1:1:1 gives the best degradation efficiency which shows the degradation of methyl orange up to 78%. Then comes the composite 1:3:1 which gives degradation efficiency upto 33% and then the composite 3:1:1 which gives least activity of only 19% which is evident from the graph.

The formula used for the calculation of % efficiency is = {(Ao – At)/Ao} x 100

Ao = absorbance at t=0 min and At = absorbance at t=t min.

4.5. Water Splitting CV analysis:

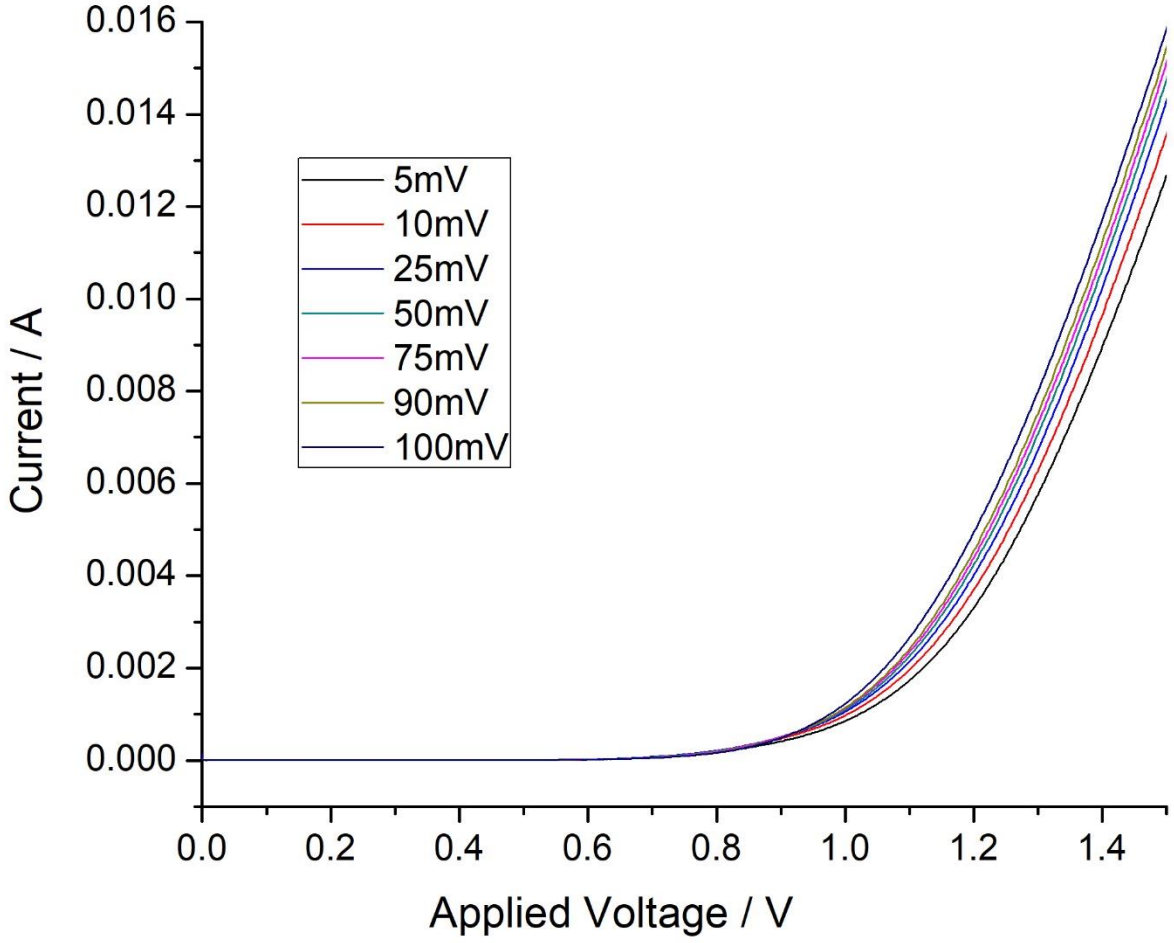

Figure 45: Scan Rate of Water Splitting CV reaction with KCL

As it is evident from the graph that as we increase the scan rate, the current is also increased and also as the scan rate increase the voltage is shifted towards higher peak and the time for the release of electron is decreased. We can see that as the current is increased from 5mV to 100mV, the voltage has also increased to a considerable level.

As the scan rate increase, the conductivity is also increased which shows the stability of the applied composite. The stability of the composite was also tested by a stability cure and it showed that the composite has a uniform morphology. The film of the composite was uniform and no change in morphology indicated a stable nano composite.

Water splitting to result hydrogen production by solar simulated xenon light radiation was successfully represented by $NiFe_2O_4$/g-C_3N_4/ZnO nano composite and the hydrogen production can be increased with increased efficiency of the nano composite and more exposure to light.

The best result was shown by the nano composite 1:1:1 which showed most stability and higher conductivity with increasing voltage which makes it clear that the hydrogen production by water splitting can be best carried out if the composite prepared by $NiFe_2O_4$, g-C_3N_4, and ZnO is in equal ratio.

Conclusion

The development of heterogeneous nano composites of nickel ferrite, graphitic carbon nitride and zinc oxide has been reported in this work. Composites of different ratios were prepared by simple solid state mixing method. Synthesized photo catalysts were then characterized by different techniques including XRD and SEM. Dye degradation experiment was carried out under Xe lamp and then checked by UV spectrophotometer. 1:1:1 composite showed the maximum activity for methyl orange with almost 80% efficiency. Water splitting was also carried out by the CV reaction which again showed the best stability and higher conductivity with scan rate for the composite 1:1:1. This concluded that the composite with ratio 1:1:1 is the most stable and hence can be used for water purification and energy production.

Future Perspectives

- The photo catalytic composites formed can also be used for degradation of other dyes as well as other organic pollutants for the purpose of water purification.
- These prepared nano composites can be used as photo voltaic cells in water splitting for the production of H_2 and other types of fuel and energy.
- New techniques can be developed to refrain from recombination of photo generated charge carriers for further photo catalytic applications in different fields.
- Different parameters and their effects can be determined such dye and catalyst concentration, effect of pH and temperature.

References:

[1] P. M. Dellamatrice, M. E. Silva-Stenico, L. A. B. de Moraes, M. F. Fiore, and R. T. R. Monteiro, "Degradation of textile dyes by cyanobacteria," *brazilian journal of microbiology*, vol. 48, pp. 25-31, 2017.

[2] L. Mun, "Degradation of dyes using zinc oxide as the photocatalyst," MS thesis, Putra University, Serdang, Malaysia, 2008.

[3] U. G. Akpan and B. H. Hameed, "Parameters affecting the photocatalytic degradation of dyes using TiO2-based photocatalysts: a review," *Journal of hazardous materials*, vol. 170, pp. 520-529, 2009.

[4] K. Kabra, R. Chaudhary, and R. L. Sawhney, "Treatment of hazardous organic and inorganic compounds through aqueous-phase photocatalysis: a review," *Industrial & engineering chemistry research*, vol. 43, pp. 7683-7696, 2004.

[5] M. R. Hoffmann, S. T. Martin, W. Choi, and D. W. Bahnemann, "Environmental applications of semiconductor photocatalysis," *Chemical reviews*, vol. 95, pp. 69-96, 1995.

[6] A. Fujishima, T. N. Rao, and D. A. Tryk, "Titanium dioxide photocatalysis," *Journal of photochemistry and photobiology C: Photochemistry reviews*, vol. 1, pp. 1-21, 2000.

[7] A. Kudo, R. Niishiro, A. Iwase, and H. Kato, "Effects of doping of metal cations on morphology, activity, and visible light response of photocatalysts," *Chemical Physics*, vol. 339, pp. 104-110, 2007.

[8] U. Diebold, "The surface science of titanium dioxide," *Surface science reports*, vol. 48, pp. 53-229, 2003.

[9] A. R. Malagutti, H. A. Mourao, J. R. Garbin, and C. Ribeiro, "Deposition of TiO2 and Ag: TiO2 thin films by the polymeric precursor method and their application in the photodegradation of textile dyes," *Applied Catalysis B: Environmental*, vol. 90, pp. 205-212, 2009.

[10] M. Ni, M. K. Leung, D. Y. Leung, and K. Sumathy, "A review and recent developments in photocatalytic water-splitting using TiO2 for hydrogen production," *Renewable and Sustainable Energy Reviews*, vol. 11, pp. 401-425, 2007.

[11] X. Yang, A. Wolcott, G. Wang, A. Sobo, R. C. Fitzmorris, F. Qian, *et al.*, "Nitrogen-doped ZnO nanowire arrays for photoelectrochemical water splitting," *Nano letters*, vol. 9, pp. 2331-2336, 2009.

[12] K. Maeda, T. Takata, M. Hara, N. Saito, Y. Inoue, H. Kobayashi, *et al.*, "GaN: ZnO solid solution as a photocatalyst for visible-light-driven overall water splitting," *Journal of the American Chemical Society*, vol. 127, pp. 8286-8287, 2005.

[13] H.-Y. Zhu, R. Jiang, Y.-Q. Fu, R.-R. Li, J. Yao, and S.-T. Jiang, "Novel multifunctional NiFe2O4/ZnO hybrids for dye removal by adsorption, photocatalysis and magnetic separation," *Applied surface science*, vol. 369, pp. 1-10, 2016.

[14] C. Borgohain, K. K. Senapati, K. Sarma, and P. Phukan, "A facile synthesis of nanocrystalline CoFe2O4 embedded one-dimensional ZnO hetero-structure and its use in photocatalysis," *Journal of Molecular Catalysis A: Chemical*, vol. 363, pp. 495-500, 2012.

[15] J. Adeleke, T. Theivasanthi, M. Thiruppathi, M. Swaminathan, T. Akomolafe, and A. Alabi, "Photocatalytic degradation of methylene blue by ZnO/NiFe2O4 nanoparticles," *Applied surface science*, vol. 455, pp. 195-200, 2018.

[16] M. Shekofteh-Gohari, A. Habibi-Yangjeh, M. Abitorabi, and A. Rouhi, "Magnetically separable nanocomposites based on ZnO and their applications in photocatalytic processes: a review," *Critical reviews in environmental science and technology*, vol. 48, pp. 806-857, 2018.

[17] V. Etacheri, R. Roshan, and V. Kumar, "Mg-doped ZnO nanoparticles for efficient sunlight-driven photocatalysis," *ACS applied materials & interfaces*, vol. 4, pp. 2717-2725, 2012.

[18] G. Zhang, W. Xu, Z. Li, W. Hu, and Y. Wang, "Preparation and characterization of multi-functional CoFe2O4–ZnO nanocomposites," *Journal of Magnetism and Magnetic Materials*, vol. 321, pp. 1424-1427, 2009.

[19] A. A. Al-Kahtani and M. F. A. Taleb, "Photocatalytic degradation of Maxilon CI basic dye using CS/CoFe2O4/GONCs as a heterogeneous photo-Fenton catalyst prepared by gamma irradiation," *Journal of hazardous materials*, vol. 309, pp. 10-19, 2016.
[20] W. Chiu, P. Khiew, M. Cloke, D. Isa, H. Lim, T. Tan, *et al.*, "Heterogeneous seeded growth: synthesis and characterization of bifunctional Fe3O4/ZnO core/shell nanocrystals," *The Journal of Physical Chemistry C*, vol. 114, pp. 8212-8218, 2010.
[21] S. Huang, Y. Xu, T. Zhou, M. Xie, Y. Ma, Q. Liu, *et al.*, "Constructing magnetic catalysts with in-situ solid-liquid interfacial photo-Fenton-like reaction over Ag3PO4@ NiFe2O4 composites," *Applied Catalysis B: Environmental*, vol. 225, pp. 40-50, 2018.
[22] Y. Ren, Q. Dong, J. Feng, J. Ma, Q. Wen, and M. Zhang, "Magnetic porous ferrospinel NiFe2O4: a novel ozonation catalyst with strong catalytic property for degradation of di-n-butyl phthalate and convenient separation from water," *Journal of colloid and interface science*, vol. 382, pp. 90-96, 2012.
[23] S. Gautam, P. Shandilya, V. P. Singh, P. Raizada, and P. Singh, "Solar photocatalytic mineralization of antibiotics using magnetically separable NiFe2O4 supported onto graphene sand composite and bentonite," *Journal of Water Process Engineering*, vol. 14, pp. 86-100, 2016.
[24] F. Dong, Z. Zhao, T. Xiong, Z. Ni, W. Zhang, Y. Sun, *et al.*, "In situ construction of g-C3N4/g-C3N4 metal-free heterojunction for enhanced visible-light photocatalysis," *ACS applied materials & interfaces*, vol. 5, pp. 11392-11401, 2013.
[25] X. Yang, F. Qian, G. Zou, M. Li, J. Lu, Y. Li, *et al.*, "Facile fabrication of acidified g-C3N4/g-C3N4 hybrids with enhanced photocatalysis performance under visible light irradiation," *Applied Catalysis B: Environmental*, vol. 193, pp. 22-35, 2016.
[26] S. Cao and J. Yu, "g-C3N4-based photocatalysts for hydrogen generation," *The journal of physical chemistry letters*, vol. 5, pp. 2101-2107, 2014.
[27] S. Yan, Z. Li, and Z. Zou, "Photodegradation of rhodamine B and methyl orange over boron-doped g-C3N4 under visible light irradiation," *Langmuir*, vol. 26, pp. 3894-3901, 2010.
[28] Q. Li, N. Zhang, Y. Yang, G. Wang, and D. H. Ng, "High efficiency photocatalysis for pollutant degradation with MoS2/C3N4 heterostructures," *Langmuir*, vol. 30, pp. 8965-8972, 2014.
[29] D. Li and H. Haneda, "Morphologies of zinc oxide particles and their effects on photocatalysis," *Chemosphere*, vol. 51, pp. 129-137, 2003.
[30] S. Morrison and T. Freund, "Chemical role of holes and electrons in ZnO photocatalysis," *The Journal of chemical physics*, vol. 47, pp. 1543-1551, 1967.
[31] J. L. Yang, S. J. An, W. I. Park, G. C. Yi, and W. Choi, "Photocatalysis using ZnO thin films and nanoneedles grown by metal–organic chemical vapor deposition," *Advanced materials*, vol. 16, pp. 1661-1664, 2004.
[32] Y. Zhang, G. Rimal, J. Tang, and Q. Dai, "Synthesis of NiFe2O4 nanoparticles for energy and environment applications," *Materials Research Express*, vol. 5, p. 025023, 2018.
[33] J. Guo, S. Zhu, Z. Chen, Y. Li, Z. Yu, Q. Liu, *et al.*, "Sonochemical synthesis of TiO2 nanoparticles on graphene for use as photocatalyst," *Ultrasonics sonochemistry*, vol. 18, pp. 1082-1090, 2011.
[34] T. A. Saleh and V. K. Gupta, "Photo-catalyzed degradation of hazardous dye methyl orange by use of a composite catalyst consisting of multi-walled carbon nanotubes and titanium dioxide," *Journal of Colloid and Interface Science*, vol. 371, pp. 101-106, 2012.
[35] M. Rashed and A. El-Amin, "Photocatalytic degradation of methyl orange in aqueous TiO2 under different solar irradiation sources," *International Journal of Physical Sciences*, vol. 2, pp. 73-81, 2007.
[36] Y. Liu, Y. Song, Y. You, X. Fu, J. Wen, and X. Zheng, "NiFe2O4/g-C3N4 heterojunction composite with enhanced visible-light photocatalytic activity," *Journal of Saudi Chemical Society*, vol. 22, pp. 439-448, 2018.
[37] G. Gebreslassie, P. Bharali, U. Chandra, A. Sergawie, P. K. Baruah, M. R. Das, *et al.*, "Hydrothermal Synthesis of g- C3N4/NiFe2O4 Nanocomposite and Its Enhanced Photocatalytic Activity," *Applied Organometallic Chemistry*, p. e5002, 2019.

[38] W. Liu, M. Wang, C. Xu, and S. Chen, "Facile synthesis of g-C3N4/ZnO composite with enhanced visible light photooxidation and photoreduction properties," *Chemical Engineering Journal,* vol. 209, pp. 386-393, 2012.
[39] Y. Qiu, K. Yan, H. Deng, and S. Yang, "Secondary branching and nitrogen doping of ZnO nanotetrapods: building a highly active network for photoelectrochemical water splitting," *Nano letters,* vol. 12, pp. 407-413, 2011.
[40] J.-X. Sun, Y.-P. Yuan, L.-G. Qiu, X. Jiang, A.-J. Xie, Y.-H. Shen, *et al.*, "Fabrication of composite photocatalyst gC 3 N 4–ZnO and enhancement of photocatalytic activity under visible light," *Dalton Transactions,* vol. 41, pp. 6756-6763, 2012.
[41] T. Peng, X. Zhang, H. Lv, and L. Zan, "Preparation of NiFe2O4 nanoparticles and its visible-light-driven photoactivity for hydrogen production," *Catalysis Communications,* vol. 28, pp. 116-119, 2012.
[42] H. S. Kim, D. Kim, B. S. Kwak, G. B. Han, M.-H. Um, and M. Kang, "Synthesis of magnetically separable core@ shell structured NiFe2O4@ TiO2 nanomaterial and its use for photocatalytic hydrogen production by methanol/water splitting," *Chemical Engineering Journal,* vol. 243, pp. 272-279, 2014.
[43] J. Domínguez-Arvizu, J. Jiménez-Miramontes, J. Salinas-Gutiérrez, M. Meléndez-Zaragoza, A. López-Ortiz, and V. Collins-Martínez, "Optical properties determination of NiFe2O4 nanoparticles and their photocatalytic evaluation towards hydrogen production," *International Journal of Hydrogen Energy,* vol. 42, pp. 30242-30248, 2017.
[44] J. Wen, J. Xie, X. Chen, and X. Li, "A review on g-C3N4-based photocatalysts," *Applied surface science,* vol. 391, pp. 72-123, 2017.
[45] Y. Panahian and N. Arsalani, "Synthesis of hedgehoglike F-TiO2 (B)/CNT nanocomposites for sonophotocatalytic and photocatalytic degradation of malachite green (MG) under visible light: kinetic study," *The Journal of Physical Chemistry A,* vol. 121, pp. 5614-5624, 2017.
[46] S. Kumar, B. Kumar, A. Baruah, and V. Shanker, "Synthesis of magnetically separable and recyclable g-C3N4–Fe3O4 hybrid nanocomposites with enhanced photocatalytic performance under visible-light irradiation," *The Journal of Physical Chemistry C,* vol. 117, pp. 26135-26143, 2013.
[47] Q. Zhang, M. Xu, B. You, Q. Zhang, H. Yuan, and K. Ostrikov, "Oxygen vacancy-mediated ZnO nanoparticle photocatalyst for degradation of methylene blue," *Applied Sciences,* vol. 8, p. 353, 2018.
[48] C. B. Ong, L. Y. Ng, and A. W. Mohammad, "A review of ZnO nanoparticles as solar photocatalysts: synthesis, mechanisms and applications," *Renewable and Sustainable Energy Reviews,* vol. 81, pp. 536-551, 2018.
[49] G. H. Munshi, A. M. Ibrahim, and L. M. Al-Harbi, "Inspired preparation of zinc oxide nanocatalyst and the photocatalytic activity in the treatment of methyl orange dye and paraquat herbicide," *International Journal of Photoenergy,* vol. 2018, 2018.
[50] H. J. Kong, D. H. Won, J. Kim, and S. I. Woo, "Sulfur-doped g-C3N4/BiVO4 composite photocatalyst for water oxidation under visible light," *Chemistry of Materials,* vol. 28, pp. 1318-1324, 2016.
[51] Y. Yao, Y. Cai, F. Lu, J. Qin, F. Wei, C. Xu, *et al.*, "Magnetic ZnFe2O4–C3N4 hybrid for photocatalytic degradation of aqueous organic pollutants by visible light," *Industrial & Engineering Chemistry Research,* vol. 53, pp. 17294-17302, 2014.
[52] J. Li, M. Zhou, Z. Ye, H. Wang, C. Ma, P. Huo, *et al.*, "Enhanced photocatalytic activity of gC 3 N 4–ZnO/HNT composite heterostructure photocatalysts for degradation of tetracycline under visible light irradiation," *RSC Advances,* vol. 5, pp. 91177-91189, 2015.
[53] S. G. Babu, R. Vinoth, B. Neppolian, D. D. Dionysiou, and M. Ashokkumar, "Diffused sunlight driven highly synergistic pathway for complete mineralization of organic contaminants using reduced graphene oxide supported photocatalyst," *Journal of hazardous materials,* vol. 291, pp. 83-92, 2015.

[54] R. L. Narayana, M. Matheswaran, A. A. Aziz, and P. Saravanan, "Photocatalytic decolourization of basic green dye by pure and Fe, Co doped TiO2 under daylight illumination," *Desalination*, vol. 269, pp. 249-253, 2011.